

Rescaled Einstein-Gauss-Bonnet Gravity Inflation

V.K. Oikonomou^{1,2,*}, Ardit Gkioni^{1,†}, Iason Sdranis^{1,‡}, Pyotr Tsyba^{2,§} and Olga Razina^{2,¶}

¹*Department of Physics, Aristotle University of Thessaloniki, Thessaloniki 54124, Greece and*

²*L.N. Gumilyov Eurasian National University - Astana, 010008, Kazakhstan*

We study the inflationary phenomenology of a rescaled Einstein-Gauss-Bonnet gravity. In this framework, the gravitational constant of the Einstein-Hilbert term is rescaled due to effective terms active in the high curvature era. Basically, the total theory is an $F(R, G, \phi)$ theory with the Gauss-Bonnet part contributing only a non-minimal coupling to the scalar field, so it is a theory with string theory origins and with a non-trivial $F(R)$ gravity part. The $F(R)$ gravity part in the high curvature regime contributes only a rescaled Einstein-Hilbert term and thus the resulting theory is effectively a rescaled version of a standard Einstein-Gauss-Bonnet theory. We develop the formalism of rescaled Einstein-Gauss-Bonnet gravity, taking in account the GW170817 constraints on the gravitational wave speed. We show explicitly how the rescaled theory affects directly the primordial scalar and tensor perturbations, and how the slow-roll and observational indices of inflation are affected by the rescaling of the theory. We perform a thorough phenomenological analysis of several models of interest and we show that it is possible to obtain viable inflationary theories compatible with the latest Planck data. Also among the studied models there are cases that yield a relatively large blue tilted tensor spectral index and we demonstrate that these models can lead to detectable primordial gravitational waves in the future gravitational wave experiments. Some of the scenarios examined, for specific values of the reheating temperature may be detectable by SKA, LISA, BBO, DECIGO and the Einstein Telescope.

PACS numbers: 04.50.Kd, 95.36.+x, 98.80.-k, 98.80.Cq, 11.25.-w

I. INTRODUCTION

One of the most refined mental perceptions of theoretical physicists about the early Universe dynamics is the inflationary paradigm [1–4], which solves fundamental problems of the Big Bang cosmology in a refined and elegant way. Also, its prospects of detection are realistic and thus it is not a vague theoretical construction that yields elegant physics. Indeed, the future Cosmic Microwave Background (CMB) experiments, like the Simons observatory [5] and hopefully the CMB stage 4 experiments [6], if these become operational, will directly probe or constraint the B -modes of the CMB. These B -modes constitute a direct probe for the primordial occurrence of the inflationary era. Apart from that, the future gravitational wave experiments [7–15] can also provide concrete information for the existence of a stochastic gravitational wave background of primordial origin. These are tests for inflation, that will hopefully yield some information about this mysterious primordial era of our Universe. It is conceivable that the verification of the inflationary era will be one of the most important achievements of theoretical physics, and of equal importance with the discovery of the Higgs particle, if not greater. The observational signs coming from NANOGrav [16] point out to the existence of a stochastic gravitational wave background, which is not certain yet whether it is of cosmological or astrophysical origin. However, in the context of inflationary theories it is hard or even impossible to explain the 2023 NANOGrav stochastic gravitational wave signal [17], and inflation in conjunction with extra physics might explain the signal see for example [18–20]. One is certain, inflation alone cannot explain the NANOGrav signal.

With regard to the inflationary paradigm, there are two mainstream descriptions, the single scalar field theory inflationary description [1–4], and the geometric realization of inflation in the context of some modified gravity [21–24]. One candidate theory that can describe efficiently the inflationary era is Einstein-Gauss-Bonnet (EGB) theory of gravity [25–51], which can actually predict a blue-tilted tensor spectral index, a feature absent in single scalar field and $f(R)$ gravity descriptions of inflation. The motivation for these theories is strong, since the EGB theories are

*Electronic address: Corresponding author: voikonomou@gapps.auth.gr; v.k.oikonomou1979@gmail.com

†Electronic address: arisgkioni@gmail.com

‡Electronic address: isdranis@protonmail.com

§Electronic address: pyotrtsyba@gmail.com

¶Electronic address: olvikraz@mail.ru

basically string theory originating theories. Indeed, if one considers that a scalar field is responsible for the inflationary dynamics, then the most general two derivative scalar field Lagrangian in four dimensions is the following,

$$\mathcal{S}_\varphi = \int d^4x \sqrt{-g} \left(\frac{1}{2} Z(\varphi) g^{\mu\nu} \partial_\mu \varphi \partial_\nu \varphi + \mathcal{V}(\varphi) + h(\varphi) \mathcal{R} \right). \quad (1)$$

The evaluation of the scalar field in its vacuum configuration, imposes the constraints that the scalar field can be either conformally coupled or minimally coupled to gravity. The quantum corrections to the above gravitational action which are also consistent with diffeomorphism invariance is [51],

$$\begin{aligned} \mathcal{S}_{eff} = \int d^4x \sqrt{-g} & \left(\Lambda_1 + \Lambda_2 \mathcal{R} + \Lambda_3 \mathcal{R}^2 + \Lambda_4 \mathcal{R}_{\mu\nu} \mathcal{R}^{\mu\nu} + \Lambda_5 \mathcal{R}_{\mu\nu\alpha\beta} \mathcal{R}^{\mu\nu\alpha\beta} + \Lambda_6 \square \mathcal{R} \right. \\ & \left. + \Lambda_7 \mathcal{R} \square \mathcal{R} + \Lambda_8 \mathcal{R}_{\mu\nu} \square \mathcal{R}^{\mu\nu} + \Lambda_9 \mathcal{R}^3 + \mathcal{O}(\partial^8) + \dots \right), \end{aligned} \quad (2)$$

where the parameters Λ_i , $i = 1, 2, \dots, 6$ are appropriate dimensionful constants. Apparently the EGB theories of gravity are a subclass of these quantum corrections. The attributes of EGB theories have been frequently studied and presented in the relevant literature [25–51]. However in 2017 the striking GW170817 event [52–55] has cast doubts on theories predicting propagation speed for tensor perturbations distinct from that of the light speed [56–60]. The remedy for EGB theories was given in a series of articles [61–63], in which it was shown that the resulting EGB theories can be compatible with the GW170817 event, if the scalar potential the EGB scalar coupling function are constrained and related in a specific way. In this work, we aim to study these viable classes of EGB theories, with the fundamental difference that gravity is stronger or weaker during the inflationary era. We call these theories rescaled EGB theories, since the Einstein-Hilbert term is rescaled by a constant number. Such rescaled EGB theories are effective theories originating possible by higher order terms of the Ricci scalar in the action, which during the early time era yield such a rescaling in the Einstein-Hilbert term. These theories are motivated from fundamental principles, since the effective Lagrangian of $f(R)$ gravity is in general dependent on basic cosmological parameters like the cosmological constant and the same $f(R)$ gravity has to describe the early and late-time eras of our Universe. So if $f(R)$ gravity is the optimal theory for describing inflation and dark energy, then effective exponential terms of the form $\lambda e^{-\Lambda/R}$ are expected to appear in the theory, where Λ is the cosmological constant. Such terms in the large curvature limit lead to terms of the form λR , so effectively, the primordial $f(R)$ gravity during inflation is a rescaled Einstein-Hilbert gravity. Now a good question is whether instabilities or ghost degrees of freedom arise in the theory. However, no such issue arises since the propagating degrees of freedom of the effective rescaled theory is the same as in ordinary $f(R)$ gravity in the presence of EGB terms. The only problematic issue is the possibility to have antigravity effects if the rescaling λR is negative and larger than R , but this can be avoided by suitably choosing the parameter λ . We will examine in detail the inflationary phenomenology of such theories, pointing out the significance of the rescaling and also we point out the cases in which the tensor spectral index acquires large values, a feature important for future gravitational wave detections. We examine several models of theoretical importance and we confront the results with the latest Planck data. Furthermore, for the models that predict a blue-tilted tensor spectrum, we evaluate the predicted energy spectrum of the primordial gravitational waves and we confront the findings with the sensitivity curves of the future and current gravitational waves experiments. As we show, the predicted energy spectrum of primordial gravitational waves from rescaled EGB gravities can be detectable in future gravitational wave experiments.

II. THE RESCALED EGB THEORETICAL FRAMEWORK

The rescaled EGB theory of gravity has the following gravitational action,

$$\mathcal{S} = \int d^4x \sqrt{-g} \left(\frac{\beta R}{2\kappa^2} - \frac{1}{2} g^{\mu\nu} \nabla_\mu \phi \nabla_\nu \phi - V(\phi) - \xi(\phi) \mathcal{G} \right), \quad (3)$$

with $\kappa = \frac{1}{M_{Pl}} = \sqrt{8\pi G}$ being the gravitational constant, M_{Pl} standing for the reduced Planck mass and β is a dimensionless constant, which quantifies the rescaling of the Einstein-Hilbert term. Such rescaled versions of EGB gravity may originate from higher order $f(R)$ gravities, with action,

$$\mathcal{S} = \int d^4x \sqrt{-g} \frac{f(R)}{2\kappa^2}. \quad (4)$$

One example of such effective $f(R)$ gravities is [64],

$$f(R) = R - \gamma \lambda \Lambda - \lambda R \exp\left(-\frac{\gamma \Lambda}{R}\right) - \frac{\Lambda \left(\frac{R}{m_s^2}\right)^\delta}{\zeta}, \quad (5)$$

which in the large curvature limit yields the following form,

$$\lambda R \exp\left(-\frac{\gamma\Lambda}{R}\right) \simeq -\gamma\lambda\Lambda - \frac{\gamma^3\lambda\Lambda^3}{6R^2} + \frac{\gamma^2\lambda\Lambda^2}{2R} + \lambda R, \quad (6)$$

therefore, the complete effective action when the curvature is high takes the form,

$$\mathcal{S} = \int d^4x \sqrt{-g} \left(\frac{1}{2\kappa^2} \left(\beta R + \frac{\gamma^3\lambda\Lambda^3}{6R^2} - \frac{\gamma^2\lambda\Lambda^2}{2R} - \frac{\Lambda}{\zeta} \left(\frac{R}{m_s^2} \right)^\delta + \mathcal{O}(1/R^3) + \dots \right) - \frac{1}{2} g^{\mu\nu} \nabla_\mu \phi \nabla_\nu \phi - V(\phi) - \xi(\phi)\mathcal{G} \right), \quad (7)$$

where $\beta = 1 - \lambda$. Note that the effective Newton's constant for these theories is distinct from the ordinary value G , so this could potentially affect the Big Bang Nucleosynthesis (BBN). However, this line of thinking is not correct, because the effective rescaled theory is valid only when the curvature is high. Thus post-inflationary and even during the reheating era, the rescaled action is no longer valid and the original action should be valid. Thus taking the dominant leading order terms in the action (7), we will start our analysis with the following action,

$$S = \int d^4x \left(\beta \frac{R}{2\kappa^2} + \frac{1}{2} (\partial_\mu \phi)(\partial^\mu \phi) - V(\phi) - \frac{1}{2} \xi(\phi)\mathcal{G} \right),$$

with

$$\mathcal{G} = R^2 - 4R_{\alpha\beta}R^{\alpha\beta} + R_{\alpha\beta\gamma\delta}R^{\alpha\beta\gamma\delta}.$$

Furthermore, it is assumed that the background metric is described by the Friedmann-Robertson-Walker (FRW) metric which is:

$$ds^2 = -dt^2 + a^2(t) \sum_{i=1}^3 (dx^i)^2,$$

where in this metric framework, $a(t)$ represents the scale factor, and the Gauss-Bonnet invariant takes the form $\mathcal{G} = 24H^2(\dot{H} + H^2)$. Upon varying the action with respect to the metric, for a general metric we obtain the following field equations for the rescaled EGB gravity.

$$\frac{\beta}{\kappa^2} G_{\mu\nu} = T_{\mu\nu}^{(\xi)} + \nabla_\mu \phi \nabla_\nu \phi - \left(\frac{1}{2} g^{\alpha\beta} \nabla_\alpha \phi \nabla_\beta \phi + V \right) g_{\mu\nu}, \quad (8)$$

with the stress-energy tensor corresponding to the EGB string corrections being $T_{\mu\nu}^{(\xi)} = -\frac{2}{\sqrt{-g}} \frac{\delta(\sqrt{-g}\xi(\phi)\mathcal{G})}{\delta g^{\mu\nu}}$ and it is equal to,

$$T_{\mu\nu}^{(\xi)} = -2 \left[\left(\frac{1}{2} \mathcal{G} g_{\mu\nu} + 4R_{\mu\alpha}R_\nu^\alpha + 4R^{\alpha\beta}R_{\mu\alpha\nu\beta} - 2R_\mu^{\alpha\beta\gamma}R_{\nu\alpha\beta\gamma} - 2RR_{\mu\nu} \right) \xi \right. \\ \left. - 4 \left(\xi^{;\alpha\beta}R_{\mu\alpha\nu\beta} - \square \xi R_{\mu\nu} + 2\xi_{;\alpha(\nu}R_{\mu)}^\alpha - \frac{1}{2} \xi_{;\mu;\nu}R \right) + 2(2\xi_{;\alpha\beta}R^{\alpha\beta} - \square \xi R) g_{\mu\nu} \right]. \quad (9)$$

Accordingly, variation of the action with respect to the scalar field yields,

$$\square \phi - V' - T^{(\xi)} = 0, \quad (10)$$

where $\square = \nabla_\mu \nabla^\mu$ and $T^{(\xi)} = \xi' \mathcal{G}$. For the FRW metric, the field equations read,

$$\frac{3\beta H^2}{\kappa^2} = \frac{1}{2} \dot{\phi}^2 + V + 12\dot{\xi} H^3 \quad (11)$$

$$\frac{2\beta \dot{H}}{\kappa^2} = -\dot{\phi}^2 + 4\ddot{\xi} H \dot{H} - 4\dot{\xi} H^3 \quad (12)$$

$$\ddot{\phi} + 3H\dot{\phi} + V' + 12\xi' H^2(\dot{H} + H^2) = 0 \quad (13)$$

At this point it is apparent how the rescaled Einstein-Hilbert term βR affects the field equations, since the rescaling parameter β already appears in the field equations (11) and (12). As we will show shortly, the rescaling parameter β affects the slow-roll indices too. Considering the inflationary era of the EGB theory, we shall work under the following slow-roll conditions:

$$\dot{H} \ll H^2, \quad \frac{\dot{\phi}^2}{2} \ll V, \quad \ddot{\phi} \ll 3H\dot{\phi} \quad (14)$$

The slow-roll conditions have no direct relation with the rescaling of the Einstein-Hilbert term. These slow-roll conditions are basically the requirement that a slow-roll era of inflation occurs and these relations are not affected at all by the rescaling. Hence the slow-roll conditions are identical for the ordinary EGB and the rescaled EGB theory. Calculations will be performed under the premise, that the gravitational wave of tensor perturbations [25],

$$c_T^2 = 1 - \frac{Q_f}{2Q_t} \quad (15)$$

is equal to unity in natural units. The functions above are, $Q_f = 8(\ddot{\xi} - H\dot{\xi})$, $Q_t = F + \frac{Q_b}{2}$, $F = \frac{\beta}{\kappa^2}$ and $Q_b = -8\dot{\xi}H$. The condition $c_T^2 = 1$ demands that $Q_f = 0$ which results in a differential equation constraining the Gauss-Bonnet scalar coupling function $\xi(\phi)$. In terms of the scalar field the above differential equation, given that $\dot{\xi} = \xi'\dot{\phi}$, is written as follows,

$$\xi''\dot{\phi}^2 + \xi'\ddot{\phi} = H\xi'\dot{\phi} \quad (16)$$

Motivated by the scalar field's slow-roll conditions, we further assume,

$$\dot{\phi} \simeq \frac{H\xi'}{\xi''} \quad (17)$$

Combination of the above equations yields,

$$\frac{\xi'}{\xi''} \simeq -\frac{1}{3H^2}(V' + 12\xi'H^4) \quad (18)$$

We are now able to express all the slow roll indices with respect to the $\frac{\xi'}{\xi''}$ ratio, while upon combining,

$$\kappa \frac{\xi'}{\xi''} \ll 1 \quad (19)$$

$$12\dot{\xi}H^3 = 12\frac{\xi'^2 H^4}{\xi''} \ll V \quad (20)$$

we can further simplify the equations of motion:

$$\beta H^2 \simeq \frac{\kappa^2 V}{3} \quad (21)$$

$$\beta \dot{H} \simeq -\frac{1}{2}\kappa^2 \dot{\phi}^2 \quad (22)$$

$$\dot{\phi} \simeq \frac{H\xi'}{\xi''} \quad (23)$$

Having generated a simplified version of the field equations, we get,

$$\frac{4\kappa^2 \xi'^2 V}{3\beta^2 \xi''} \ll 1 \quad (24)$$

an approximation, which will be employed in the simplification of the slow-roll indices' expressions, starting with our initial differential equation of the scalar coupling function $\xi(\phi)$, which becomes,

$$\beta^2 \frac{V'}{V^2} + \frac{4\kappa^4}{3} \xi' \simeq 0 \quad (25)$$

Equation (25) connects the scalar coupling function $\xi(\phi)$ with the inflationary potential $V(\phi)$, which will be of paramount importance for the analysis that follows. Recalling the definitions of the slow-roll indices [25],

$$\epsilon_1 = -\frac{\dot{H}}{H^2}, \quad \epsilon_2 = \frac{\ddot{\phi}}{H\dot{\phi}}, \quad \epsilon_3 = \frac{\dot{F}}{2HF}, \quad \epsilon_4 = \frac{\dot{E}}{2HE}, \quad \epsilon_5 = \frac{\dot{F} + Q_a}{2HQ_t}, \quad \epsilon_6 = \frac{\dot{Q}_t}{2HQ_t}, \quad (26)$$

with $F = \frac{\partial F}{\partial R} = \frac{\beta}{\kappa^2}$ and E defined as ,

$$E = \frac{F}{\dot{\phi}^2} \left(\dot{\phi}^2 + 3 \left(\frac{\dot{F} + Q_a^2}{2Q_t} \right) \right) \quad (27)$$

whereas the Q_i functions are given by [25],

$$Q_a = -4\dot{\xi}H^2, \quad Q_b = -8\dot{\xi}H, \quad Q_t = F + \frac{Q_b}{2}, \quad Q_e = 16\dot{\xi}\dot{H} \quad (28)$$

$$Q_a = -4\frac{\xi'^2}{\xi''} \left(\frac{\kappa^2 V}{3\beta} \right)^{3/2}, \quad Q_b = -\frac{8\kappa^2 \xi'^2 V}{3\xi''\beta}, \quad Q_t = \frac{\beta}{\kappa^2} \left(1 - \frac{4\kappa^4 \xi'^2 V}{3\xi''\beta^2} \right), \quad Q_e = 16\frac{\xi'^3}{\xi''^2} H^2 H' \quad (29)$$

Applying the equations of motion relating H, \dot{H} to the $\frac{\xi'}{\xi''}, V(\phi)$ we obtain:

$$\epsilon_1 \simeq \frac{\kappa^2}{2\beta} \left(\frac{\xi'}{\xi''} \right)^2 \quad (30)$$

$$\epsilon_2 \simeq 1 - \epsilon_1 - \frac{\xi'\xi'''}{\xi''^2} \quad (31)$$

$$\epsilon_3 = 0 \quad (32)$$

$$\epsilon_4 \simeq \frac{\xi'}{2\xi''} \frac{E'}{E} \quad (33)$$

$$\epsilon_5 \simeq -\frac{\epsilon_1}{\lambda} \quad (34)$$

$$\epsilon_6 \simeq \epsilon_5 (1 - \epsilon_1) \quad (35)$$

whereby the explicit forms of the $E(\phi)$ and assisting $\lambda(\phi)$ function are,

$$E(\phi) = \frac{\beta}{\kappa^2} + \frac{8\kappa^4 \xi'^2 V^2}{3\beta^2 \left(1 - \frac{4\kappa^4 \xi'^2 V}{3\beta^2 \xi''} \right)} \quad (36)$$

$$\lambda(\phi) = \frac{3\beta}{4\kappa^2 \xi'' V} \quad (37)$$

It is apparent at this point that the rescaling parameter β affects directly the slow-roll parameters, since it appears explicitly in the first slow-roll index in Eq. (30) and implicitly in the rest of the slow-roll indices, via $E(\phi)$ and λ which contain the rescaling parameter β .

The above definitions of the slow-roll indices allow for a simplified representation of the observable quantities, namely the spectral indices of the scalar and tensor primordial perturbations, which are [25],

$$n_S = 1 - 4\epsilon_1 - 2\epsilon_2 - 2\epsilon_4 \quad (38)$$

$$n_{\mathcal{T}} = -2(\epsilon_1 + \epsilon_6) \quad (39)$$

while the tensor-to-scalar ratio is equal to,

$$r = 16 \left| \left(\frac{\kappa^2 Q_e}{4H} - \epsilon_1 \right) \frac{2c_A^3}{2 + \kappa^2 Q_b} \right| \quad (40)$$

$$c_A^2 = 1 + \frac{Q_a Q_e}{3Q_a^2 + \dot{\phi}^2 \left(\frac{2}{\kappa^2} + Q_b \right)} \quad (41)$$

with c_A denoting the speed of sound for the scalar perturbations. The detailed derivation of the final forms of the observational indices and of the sound speed given in Eqs. (39)-(41) can be found in Ref. [25]. Lastly, this framework allows us to express the number of e -foldings in terms of the scalar field. Given ϕ_i and ϕ_f the field values at the first horizon crossing and at the end of inflation respectively, the number of e -foldings is,

$$N = \int_{t_i}^{t_f} H dt = \int_{\phi_i}^{\phi_f} \frac{H}{\dot{\phi}} dt = \int_{\phi_i}^{\phi_f} \frac{\xi''}{\xi'} d\phi \quad (42)$$

III. EBG INFLATIONARY PHENOMENOLOGY

In this section, we delve further into detailed calculations of slow-roll and scalar/tensor perturbation spectral indices for candidate potentials $V(\phi)$ that can realize an inflationary era. The models will be compared to the Planck data [65], which indicate that,

$$n_S = 0.9649 \pm 0.0042, \quad r < 0.064 \quad (43)$$

Also we shall compare the results with the BICEP/Keck updates on the Planck data [66] which constrain the tensor-to-scalar ratio to be $r < 0.036$ at 95% confidence. For further compatibility with the aforementioned data, values of the tensor spectral index which are positive $n_{\mathcal{T}} > 0$ will be considered prime candidates to support the inflationary regime described by our theory. In total, six candidate potentials $V(\phi)$ will be tested out, in hopes of reproducing blue-tilted values of the spectral and index, as well as the tensor-to-scalar ratio value. Furthermore, we would like to achieve these results with simultaneous compatibility with the 2018 Planck data.

A. Model I: Power law choice for $V(\phi)$

In this scenario, the simplest example of an inflationary potential is considered,

$$\xi(\phi) = \delta(\kappa\phi)^\nu \quad (44)$$

where δ is a parameter of dimension

$$[\delta] = [m]^0 \quad (45)$$

as it follows from $[R] = [m]^{-2}$ thus $\mathcal{G} \propto R^2 \Rightarrow [\mathcal{G}] = [m]^{-4}$ and $\kappa = \frac{1}{M_p}$ being the reciprocal of the Planck mass. The corresponding potential follows from Eq. (25),

$$V(\phi) = \frac{3\beta^2}{4\delta\kappa^4(\kappa\phi)^\nu + 4\kappa^4\gamma} \quad (46)$$

where γ is a dimensionless integration constant. It is noteworthy, that the addition of a factor γ to the potential has been implemented for the solemn purpose of avoiding irregular behavior around $\phi = 0$. As such, a phase tilt will bear no significant effect to the collective phenomenon. At this point, the slow roll indices are evaluated,

$$\epsilon_1 = \frac{\kappa^2 \phi^2}{2\beta(\nu - 1)^2} \quad (47)$$

$$\epsilon_2 = -\frac{\kappa^2 \phi^2}{2\beta(\nu - 1)^2} - \frac{\nu - 2}{\nu - 1} + 1 \quad (48)$$

$$\epsilon_3 = 0 \quad (49)$$

$$\epsilon_4 = \frac{\xi'}{2\xi''} \frac{\mathcal{E}'}{\mathcal{E}} \quad (50)$$

$$\epsilon_5 \simeq -\frac{2\kappa^2\xi'^2V}{3\beta^2\xi''} \quad (51)$$

$$\epsilon_6 \simeq \frac{2\kappa^2\xi'^2V}{3\beta^2\xi''} \left(1 - \frac{\kappa^2}{2\beta} \left(\frac{\xi'}{\xi''} \right)^2 \right) \quad (52)$$

$n_{\mathcal{S}}$, $n_{\mathcal{T}}$ and r which are of importance are equally as complicated and rather inelegant in their expressions, hence why they have been omitted from being presented. In order to evaluate the above indices at the first horizon crossing, recalling that ϕ_f and ϕ_i are connected via the number of e -foldings relation (42) we start by finding the scalar field value at the end of the inflationary period, characterized by $\epsilon_1 = 1$. Without the necessity of approximations, we obtain $\phi_f = \frac{\sqrt{2\beta}(\nu-1)}{\kappa}$ and thus the initial scalar field value being $\phi_i = \frac{\sqrt{2\beta}(\nu-1)e^{-\frac{N}{\nu-1}}}{\kappa}$. At this value, the spectral indices pertaining to our framework are expressed as complicated relations for which we have evaluated using code. To better grasp the $n_{\mathcal{S}}$, $n_{\mathcal{T}}$ and r dependency on the dimensionless parameters δ, γ, ν as well as the new Ricci scalar coupling β , we considered four sets of values, listed in (53).

$$\text{set 1 : } \nu = 21, \quad \gamma = 5768 \quad (53)$$

$$\text{set 2 : } \nu = 19, \quad \gamma = 57 \quad (54)$$

$$\text{set 3 : } \nu = 19, \quad \gamma = 5 \quad (55)$$

$$\text{set 4 : } \nu = 21, \quad \gamma = 7.7 \times 10^8 \quad (56)$$

Let us proceed by examining the dependence of $n_{\mathcal{S}}(\phi_i)$ in terms of (β, δ) , the Ricci coupling and the power-law model coefficient, in the parameter set 1 appearing in Eq. (53). Assuming the number of e -folds to be $N \simeq 60$, evaluating the spectral indices of primordial perturbations at the first horizon crossing, for each set of parameters at a time, yields the $n_{\mathcal{S}}$ contour plots appearing in Fig. 1. So far, the graphs point towards optimistic results in regards to a blue-tilted, rescaled Einstein-Gauss-Bonnet gravity for which $\beta = 1$ would reduce to the usual EGB framework. Another noteworthy observation consists of the influence of the dimensionless γ parameter that was added as an integration constant on the range of the potential's coefficient δ for which the 2018 Planck constraints are satisfied. A direct behavior cannot be deduced immediately, as both (γ, ν) parameters exert their influence on the variation but we may view the respective qualitative and quantitative behavior in Figs. 2, 3 and 4. At this point, we should be concerning ourselves with the prospect of such a model potential yielding a blue-tilt in its tensor spectral index of primordial perturbations with simultaneous compatibility with the 2018 Planck constraints. In Table I, we've handpicked some arbitrary values of (δ, β) that respect the aforementioned constraints and have been by the contours of Figs. 2, 3 and 4. The results are listed in Table I. As it can be seen in Table I, the model is compatible with the Planck data but also with the recent BICEP/Keck data [66], and only the set 1 is not compatible with the BICEP/Keck data. Furthermore, as it can be seen in Table I, the set 2 and set 4 produce a significant blue tilted tensor spectrum while

	δ	β	$n_{\mathcal{S}}$	$n_{\mathcal{T}}$	r
Set 1	18	0.9	0.966	0.08	0.0396
Set 2	$4.63 \cdot 10^7$	0.25	0.966	0.56	0.020
Set 3	25	0.6	0.966	0.035	0.020
Set 4	$2.48 \cdot 10^5$	0.725	0.966	0.428	0.0396

TABLE I: Validity of a blue-tilted regime for Power Law Inflation, accounting for different data Sets and free-parameter values

simultaneously being compatible with the Planck and the BICEP/Keck constraints. In addition, in Fig. 5 we confront model I with the Planck 2018 likelihood curves. As it can be seen, the model is nicely fitted in the Planck likelihood

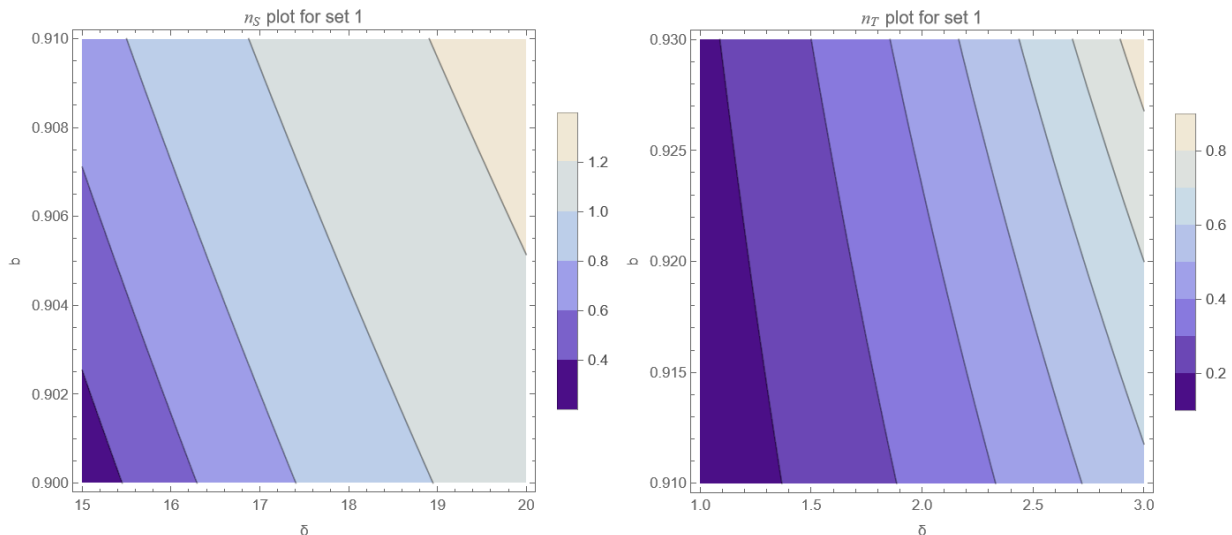


FIG. 1: The spectral indices for the free parameters of data Set 1 of our theory. Note that in each scenario, the indices respect the 2018 Planck constraints on specific contour curves of n_s , yet in each scenario they yield a blue-tilted n_T and respect the constraints we've imposed. The same analysis will follow for the rest of the data Sets, but the same behavior should be the case for the rest of the data Sets.

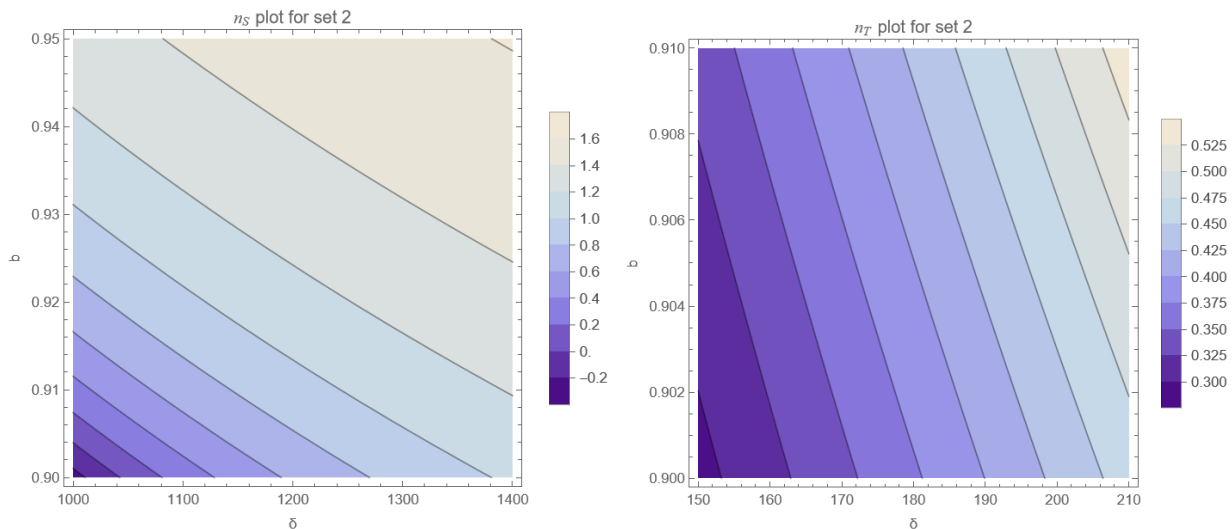


FIG. 2: The spectral indices for the free parameters of data Set 2 of our theory. Note the similar variations of both spectral indices with the previous set and the blue-tilt that they commonly result in.

curves. We need to note here that the Planck data do not directly constrain the tensor spectral index because there is no detection of tensor modes at all. There are the LIGO-Virgo constraints on the tensor spectral index, which are taken into account in a later section, but still these are too restrictive to constrain the tensor spectral index for large frequency range starting from the LIGO-Virgo operational frequencies down to the Litebird frequencies. The reason is that a broken power-law behavior is expected to apply in these frequencies, as discussed in Ref. [67]. Also it is noticeable that the rescaling parameter β plays an important role since it allows a great diversity in the choice of free parameters and a diversity in the viable inflationary phenomenologies. The only remaining feature to attest to, is the validation of the slow-roll approximation regime which we have assumed to hold true throughout our entire analysis. In essence, this requires that for all of the above parameter sets and (δ, β) values, the conditions imposed slow-roll conditions of the previous section are fully respected. Starting with the very first set of parameters, for the sake of providing the process of validation, the condition (14) which is equivalent to requiring $\epsilon_1 \ll 1$ holds true as for the 1st set of values it is of the order $\mathcal{O}(10^{-7})$, $\frac{\dot{\phi}^2}{2V} \simeq 10^{-69}$, $\epsilon_2 \simeq \mathcal{O}(10^{-2})$ and the theory's $\kappa \frac{\xi'}{\zeta''}$ ratio is of order

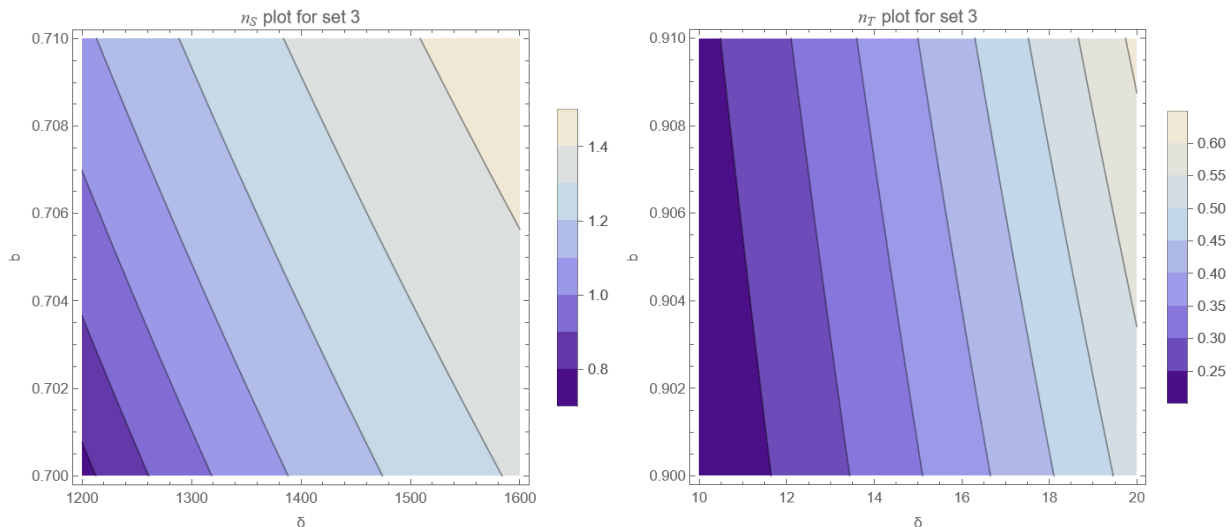


FIG. 3: The spectral indices for the free parameters of data Set 3 of our theory. It is immediately noted how the free parameters alter the domain of satisfaction of the desired constraints.

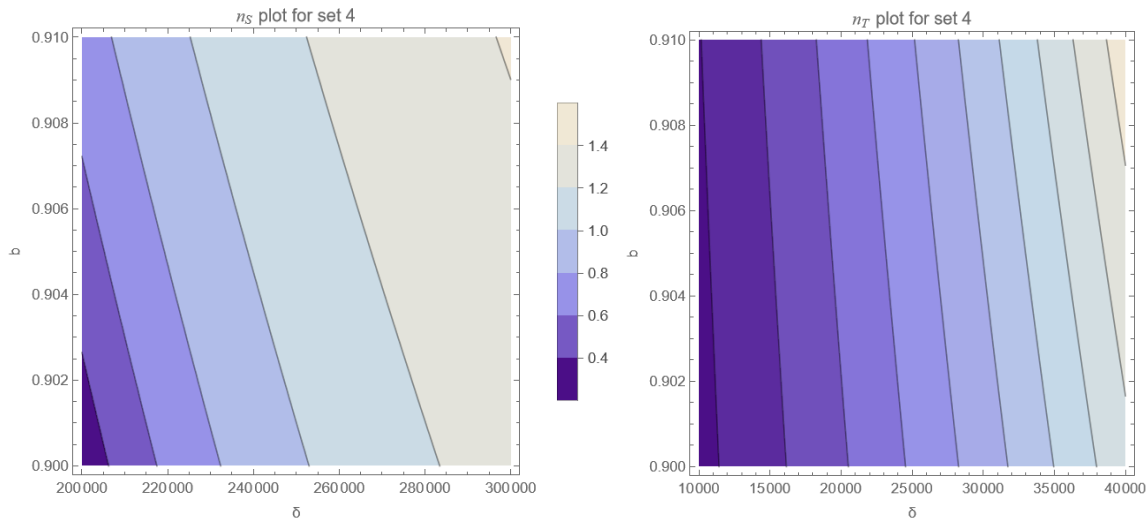


FIG. 4: The spectral indices for the free parameters of data Set 4 of our theory.

$\mathcal{O}(10^{-3})$ while the ensuing approximation for the further simplification of the higher-order slow-roll indices becomes $\frac{4\kappa^4 \xi'^2 V}{3\beta^2 \xi''} \simeq \mathcal{O}(10^{-50})$. Therefore, not only have we managed to achieve compatibility with the 2018 Planck constraints and slow-roll approximating conditions but there exists substantial evidence of a blue-tilt in the tensor spectral index n_T of primordial perturbations, especially in Sets 2-4. Before closing this section let us discuss an important issue having to do with the super-Planckian values of the scalar field in the context of the model studied in this section. The model I contains super-Planck values of the scalar field in order for it to be viable, indeed for example the final value of the scalar field at the end of inflation for this model is $\phi_f = \frac{\sqrt{2\beta}(\nu-1)}{\kappa}$, so for set 1 we have $\phi_f \sim 12.7 M_p$ which is strongly super-Planckian. This feature is due to the stringy origin of the EGB theory, and a detection of tensor spectral index so large as in the context of this model, could be a strong indication that the theory behind inflation contains string corrections. It would thus be a direct probe of string theory or even quantum gravity, at least indirect.

The super-Planck values of the scalar field are also a probe of quantum gravity or string effects, for example the Lyth bound [68] indicates that,

$$\frac{\Delta\phi}{M_p} \geq \left(\frac{r}{8}\right)^{1/2} N$$

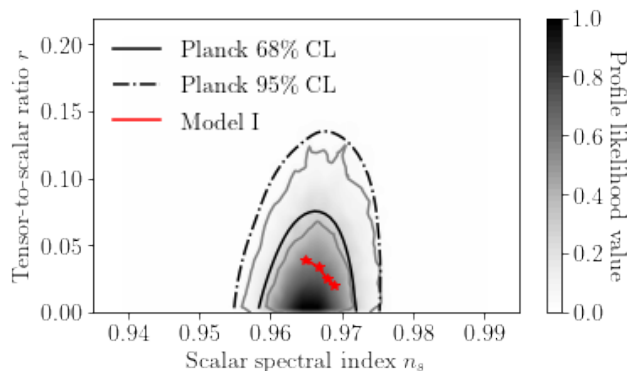


FIG. 5: The phenomenology of model I confronted with the Planck 2018 likelihood curves for various optimal values of the free parameters.

where N is the e -folding number. By taking $N \sim 60$ a future detection of the B -modes with $r \sim 0.03$ would indicate that the distance travelled by the inflaton would be $\Delta\phi \sim 3.67 M_p$ which is super-Planckian. Even a smaller r for example $r \sim 0.003$ would yield $\Delta\phi \sim 1.1619 M_p$.¹ Such a detection of B -modes would thus be an indicator of some stringy origin of the underlying theory. Although perturbation theory may not break down, however the Trans-Planckian issues might cause theoretical inconsistencies in the theoretical framework. We need to note though that the Lyth bound and the Trans-Planckian issues were derived for minimally coupled theories and not for EGB theories. Thus one must be cautious regarding these issues, and a correct treatment would be required to extend the bounds for EGB theories. However a strong blue tilt is related with super-Planckian values of the scalar field in the context of EGB and would thus be a strong hint for a stringy origin of the underlying theory.

B. Model II: Arctangent choice for $V(\phi)$

In this scenario, we examine the compatibility of inflation by an Arctan-driven potential,

$$V(\phi) = \frac{1}{\kappa^4} \left[1 - \frac{2}{\pi} \arctan \left(\frac{\phi}{\mu} \right) \right] \quad (57)$$

This one free-parameter model was initially considered in order to extensively study the accuracy, with which the first and second slow-roll order power spectra can approximate the actual power spectrum of the inflationary cosmological perturbations. Once again, solving Eq. (25) results in a Gauss-Bonnet coupling constant of the form,

$$\xi(\phi, \mu) = -\frac{3\beta^2}{4} + \frac{3\beta^2}{4 \left(1 - \frac{2}{\pi} \arctan \left(\frac{\phi}{\mu} \right) \right)} \quad (58)$$

It is to be highlighted that, in this instance, the slow-roll indices obtain quite complicated expressions, due to the nature of $\xi(\phi, \mu)$ derivatives, which we will not quote here for brevity. Solving $\epsilon_1 = 1$ exactly is arduous and hardly possible, which is precisely why the calculations were performed up to $\mathcal{O}(3)$ in terms of ϕ , yielding the following functional form of the ϵ_1 slow-roll index,

$$\epsilon_1(x) \simeq \frac{0.308\kappa^2\mu^2}{\beta} + \frac{0.574\kappa^2\mu\phi}{\beta} + \frac{1.170\kappa^2\phi^2}{\beta} + \mathcal{O}(\phi^3) \quad (59)$$

where convergence implies that the value of the ensuing ration $\frac{\phi}{\mu} \ll 1$ or equivalently that we're considering a specific range of the model's free parameter. Regardless, the scalar field value at the end of inflation reads,

$$\phi_f \simeq = -0.245\mu + 0.045\sqrt{10^{18}\beta - 97.4\mu^2} \quad (60)$$

¹ See also the discussion on page 16 of [69].

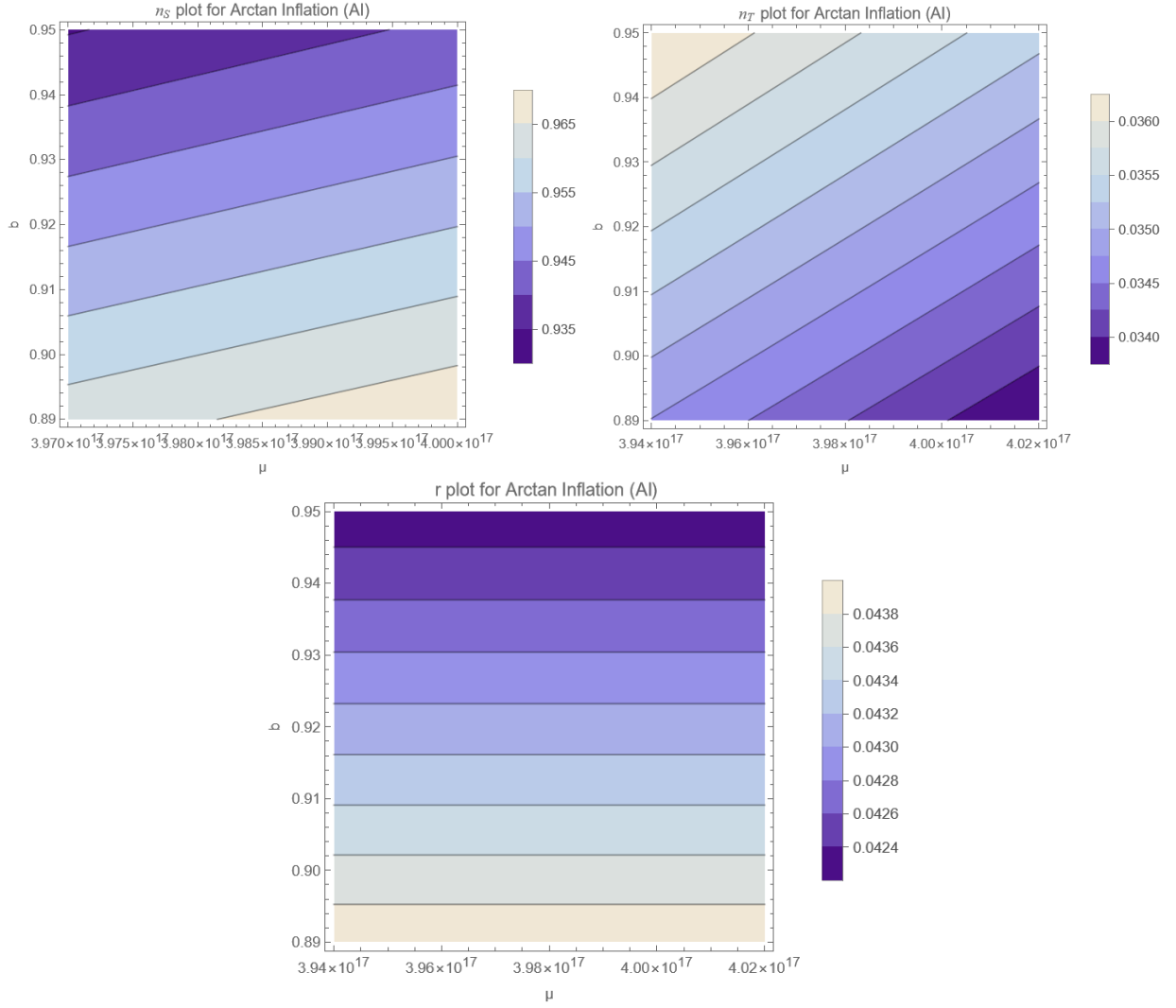


FIG. 6: The spectral indices for the free parameter of the theory as well as the rescaling factor of the EBG framework. Note that in each scenario, the indices respect the 2018 Planck constraints and yield a positive value for the tensor spectral index, albeit no higher than $n_T = 0.052$. Regardless, it is of tremendous importance that both $n_S = 0.966$ and $r < 0.064$ are respected simultaneously, however the BICEP/Keck constraints [66] are not respected for the chosen values of the free parameters. There exist values that are also compatible with the BICEP/Keck constraints, see for example Table II.

$$\phi_i = -1.57\mu \quad (61)$$

Before proceeding with the spectral indices plots, it is important to consider the limitations of the model at hand. Without any approximations to the function form of $(\xi(\phi), \epsilon_1(\phi))$ the end of inflation provided by $\epsilon_1 = 1$ will depend solely on (μ, β) . In that scenario, cases where:

$$\epsilon_2^{max} \gtrsim \epsilon_1^{max} \quad (62)$$

where by maximum we denote the slow-roll values at ϕ_{max} , then the slow-roll framework breaks down and cannot accurately describe the dynamics of inflation. Due to the odd symmetry of the potential about $x \rightarrow -x$ translations, negative values as above are accepted, resulting in $V(\phi) > 0$ altogether. Before proceeding with the plots, it will be made clear that for illustrative and qualitative purposes the range of the parameters are set to best display the characteristics of each index. As such, in the simultaneous compatibility check it will be evident that the parameter range contributes insignificantly to the end results. Therefore, the spectral indices for the arctangent framework are displayed in Fig. 6. It is to be noted, that both tensor and scalar spectral indices exhibit values that correspond to a blue-tilted inflationary regime. Moreover, by examining the compatibility with the rest of the spectral indices we gathered the viable phenomenologies in Table II. Despite the spectral yield of tensor perturbations not being as

	μ	β	n_S	n_T	r
Set 1)	$3.8 \cdot 10^{18}$	0.89	0.966	0.0348	$7.6 \cdot 10^{-17}$
Set 2)	$3.475 \cdot 10^{17}$	0.7	0.966	0.035	$9 \cdot 10^{-18}$
Set 3)	$2.672 \cdot 10^{17}$	0.6	0.966	0.035	$1.4 \cdot 10^{-17}$
Set 4)	$1.32 \cdot 10^{17}$	0.1	0.966	0.034	$1.33 \cdot 10^{-18}$

TABLE II: Validity of a blue-tilted n_T inflationary regime for an Arctangent-driven potential, accounting for various values of the rescaling and the model's free parameter.

	μ	β	ϵ_1	$\frac{\dot{\phi}^2}{2V}$	ϵ_2	$\kappa \frac{\xi'}{\xi^{\prime\prime}}$	$\frac{4\kappa^4 \xi^{\prime\prime 2} V}{3\beta^2 \xi^{\prime\prime}}$
Set 1)	$3.8 \cdot 10^{18}$	0.89	$\mathcal{O}(10^1)$	$\mathcal{O}(10^{-1})$	$\mathcal{O}(10^{-1})$	$\mathcal{O}(10^1)$	$\mathcal{O}(10^{-2})$
Set 2)	$3.475 \cdot 10^{17}$	0.7	$\mathcal{O}(10^{-2})$	$\mathcal{O}(10^{-3})$	$\mathcal{O}(10^{-1})$	$\mathcal{O}(10^{-1})$	$\mathcal{O}(10^{-2})$
Set 3)	$2.672 \cdot 10^{17}$	0.6	$\mathcal{O}(10^{-3})$	$\mathcal{O}(10^{-3})$	$\mathcal{O}(10^{-1})$	$\mathcal{O}(10^{-2})$	$\mathcal{O}(10^{-2})$
Set 4)	$1.32 \cdot 10^{17}$	0.1	$\mathcal{O}(10^{-2})$	$\mathcal{O}(10^{-3})$	$\mathcal{O}(10^{-1})$	$\mathcal{O}(10^{-2})$	$\mathcal{O}(10^{-2})$

TABLE III: Validity of the slow-roll approximations of equations (4.8) and (4.16)-(4.18). Notice how only one case scenario does not meet the necessary prerequisites.

significantly large as in the power-law scenario, it still consists of a blue-tilt and a step forward in terms of progression. We may finalize the analysis of this model only after providing the slow-roll approximation accordance with the selected values, as listed in Table III. As it can be seen, both the Planck and the BICEP/Keck constraints are respected for this model too. Parameter set 1 is not in accordance with the slow-roll demands as it is way out of the slow-roll range $\epsilon_1 > 1$, hence its omittance from compatible sets. In addition, in Fig. 7 we confront model II with the Planck 2018 likelihood curves for various suitably chosen values of the free parameters. As it can be seen, the model is nicely fitted in the Planck likelihood curves and the model is phenomenologically fitted in the sweet spot of the Planck data.

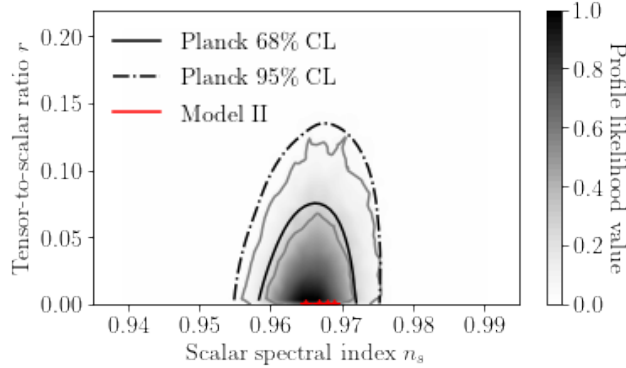


FIG. 7: The phenomenology of model II confronted with the Planck 2018 likelihood curves for various optimal values of the free parameters.

C. Model III: Double-Well Inflation for $V(\phi)$

In this model, we examine another one-parameter potential, the "Double-Well" or "Mexican hat" case which was first introduced by Goldstone as a candidate for symmetry breaking. However, in the inflationary framework it is employed to investigate the formation and structure of topological defects in spacetime. The potential reads,

$$V(\phi) = \frac{1}{k^4} \left[\left(\frac{\phi}{\mu} \right)^2 - 1 \right]^2 \quad (63)$$

with $[\mu] = [m]$ and its respective non-minimally coupling function $\xi(\phi)$ will be deduced from (25),

$$\xi(\phi) = \frac{3b^2}{4 \left[\left(\frac{\phi}{\mu} \right)^2 - 1 \right]^2} \quad (64)$$

Regarding the presentation of the slow-roll indices despite their lengthy expressions, as per usual, we've obtained,

$$\epsilon_1 \simeq \frac{\kappa^2 \phi^2 (\phi^2 - \mu^2)^2}{2\beta (5\phi^2 + \mu^2)^2} \quad (65)$$

$$\epsilon_2 \simeq - \frac{\left(\kappa^2 \phi^2 (\phi^2 - \mu^2)^2 + 2\beta (5\phi^4 + 8\phi^2 \mu^2 - \mu^4) \right)}{2\beta (5\phi^2 + \mu^2)^2} \quad (66)$$

$$\epsilon_3 \simeq 0 \quad (67)$$

$$\epsilon_4 \simeq \frac{24\beta \phi^2 (5\phi^6 + 7\phi^4 \mu^2 + 11\phi^2 \mu^4 + \mu^6)}{(\phi^2 + \mu^2) (5\phi^2 + \mu^2) \left(\kappa^2 (\phi^2 - \mu^2)^2 (\phi^2 + \mu^2) + 24\beta \phi^2 (5\phi^2 + \mu^2) \right)} \quad (68)$$

$$\epsilon_5 \simeq - \frac{2\phi^2}{\phi^2 + \mu^2} \quad (69)$$

$$\epsilon_6 \simeq \frac{4\mu^2 \phi^2 (\phi^2 - \mu^2)}{(\mu^2 + \phi^2) (\mu^2 + 5\phi^2)^2} \quad (70)$$

thereby proceed to evaluate the initial modes entering the Hubble horizon by finding the end of inflation through $\epsilon_1 = 1$ up to $\mathcal{O}(3)$ this time then we find,

$$\phi_i = \frac{\left(9\beta^{13/2} \left(\frac{1}{\kappa^2} \right)^{3/2} (6\beta + \kappa^2 \mu^2) + \zeta(\mu, \beta) \right)^{2/3} - \sqrt[3]{2} e^{40} \beta^4 \mu^2}{3 \sqrt[6]{2} e^{20} \beta^2 \sqrt[3]{9\beta^{13/2} \left(\frac{1}{\kappa^2} \right)^{3/2} (6\beta + \kappa^2 \mu^2) + \zeta(\mu, \beta)}} \quad (71)$$

$$\zeta(\mu, \beta) = \frac{\beta^{12} (2916\beta^3 + 972\beta^2 \kappa^2 \mu^2 + 81\beta \kappa^4 \mu^4 + 2e^{120} \kappa^6 \mu^6)}{\kappa^6} \quad (72)$$

Taking into consideration that the slow-roll regime for this potential is valid only for super-Planckian values of the inflaton field, the exact same problem that was encountered in the arctangent case, we demand the very weak (by cosmological standards) condition that the value of $\epsilon_2(0) < 1$, in other words ,

$$k \cdot \mu > 2\sqrt{2} \Rightarrow \mu > 2\sqrt{2} \cdot \mathcal{M}_{Pl} \quad (73)$$

With the constraints in mind, evaluation of the spectral indices at the first horizon crossing yields the plots of Fig. 8. Therefore, since has been shown that a blue-tilted inflation takes place in the super-Planckian region of values of the scalar field what remains is to validate the slow-roll approximations for this theory. Much like in every other scenario investigated so far, we will consider four different data sets yielding a blue-tilt and construct a table containing the orders of magnitude for each slow-roll approximating condition. All of the results are present in Table IV. On a last note, we also add the respective values of the spectral indices of the primordial perturbation to get a qualitative overview of our results, presented in Table V. As it can be seen, both the Planck and the BICEP/Keck constraints [66] are respected for this model too. A brief overview of the results may be synopsised in the graph of Fig. 9, where the tensor spectral index may exhibit a blue-tilt that is in accordance with the imposed Planck constraints , Finally, in Fig. 10 we confront model III with the Planck 2018 likelihood curves for various suitably chosen values of the free parameters. In this case too, the model is nicely fitted in the Planck likelihood curves and some values of the free parameters put the model predictions in the sweet spot of the Planck data.

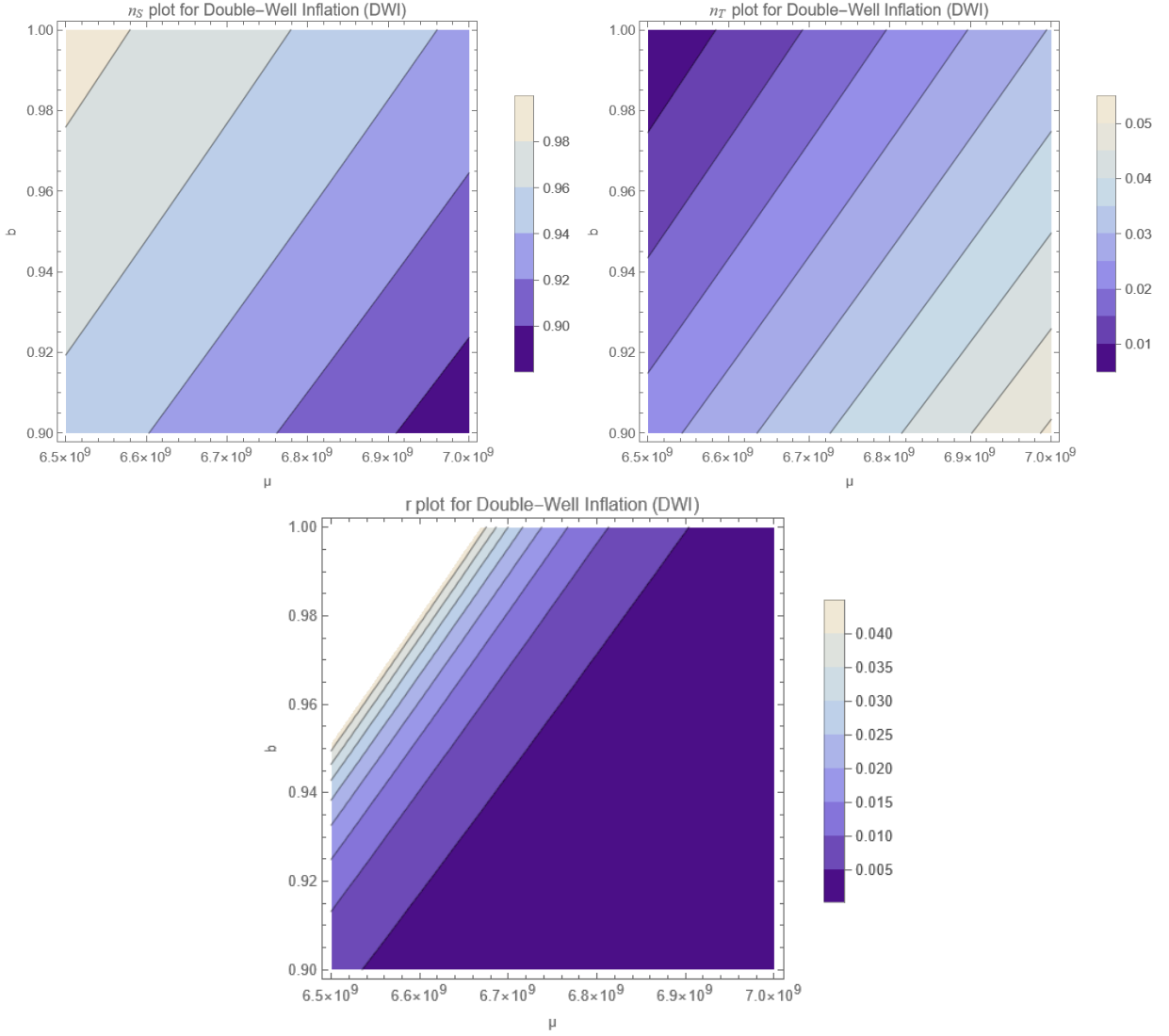


FIG. 8: The above pictures portray the qualitative and quantitative trends of the spectral indices of primordial perturbations, for a range of values within the margins of 2018 Planck compatibility and, possibly, blue-tilt of n_T . It is important to note that the values of the tensor-to-scalar ratio of the perturbation's amplitudes have been rescaled as $r' \rightarrow 10^{14}r$ in order to display its features in a palpable fashion, whereas the values of μ are of the order $10^9 \cdot GeV$.

	$\mu(10^9 \cdot GeV)$	β	ϵ_1	$\frac{\dot{\phi}^2}{2V}$	ϵ_2	$\kappa \frac{\xi'}{\xi''}$	$\frac{4\kappa^4 \xi'^2 V}{3\beta^2 \xi''}$
Set 1)	6.5	0.92	$\mathcal{O}(10^{-21})$	$\mathcal{O}(10^{-22})$	$\mathcal{O}(10^{-1})$	$\mathcal{O}(10^{-11})$	$\mathcal{O}(10^{-1})$
Set 2)	6.6	0.94	$\mathcal{O}(10^{-21})$	$\mathcal{O}(10^{-21})$	$\mathcal{O}(10^{-1})$	$\mathcal{O}(10^{-11})$	$\mathcal{O}(10^{-1})$
Set 3)	6.7	0.98	$\mathcal{O}(10^{-21})$	$\mathcal{O}(10^{-22})$	$\mathcal{O}(10^{-1})$	$\mathcal{O}(10^{-11})$	$\mathcal{O}(10^{-1})$
Set 4)	6.9	1	$\mathcal{O}(10^{-21})$	$\mathcal{O}(10^{-21})$	$\mathcal{O}(10^{-1})$	$\mathcal{O}(10^{-11})$	$\mathcal{O}(10^{-2})$

TABLE IV: Validity of the slow-roll approximations for the Double-Well Inflation (DWI)

D. Model IV: Natural Inflation model for $V(\phi)$ (NI)

Natural inflation was first proposed as an attempt to solve the fine-tuning problem of inflation, and it is closely related to axion fields [70–72]. In particular, in order to obtain sufficient inflation and the correct normalization for the microwave background anisotropies, the potential $V(\phi)$ of the inflaton must be sufficiently flat. Since we are only interested in verifying whether or not this model can reproduce blue-tilted spectral indices, the main focus will be on

	$\mu(10^9 \cdot GeV)$	β	n_S	n_T	$r(10^{-14})$
Set 1)	6.5	0.92	0.966	0.02	0.015
Set 2)	6.6	0.94	0.964	0.025	0.0012
Set 3)	6.7	0.98	0.968	0.03	0.001
Set 4)	6.9	1	0.965	0.051	0.005

TABLE V: Values of the spectral indices under the rescaled EGB framework, for the Double-Well Inflation. Note how blue-tilt is achieved in each case, with simultaneous compatibility with the 2018 Planck constraints regarding $n_S \simeq 0.966$ as well as $r < 0.064$. Thus both the Planck and the BICEP/Keck constraints [66] are respected for this model too.

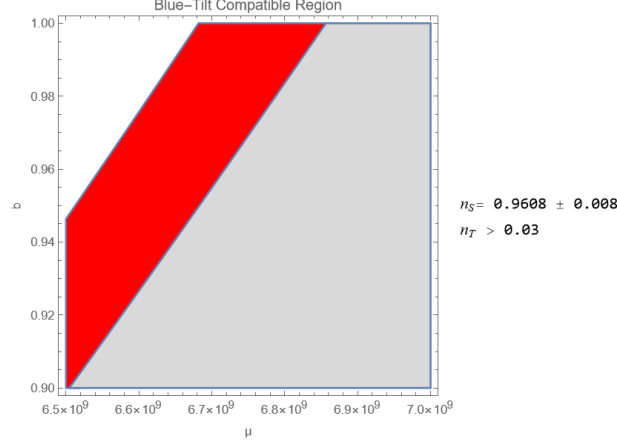


FIG. 9: Blue tilt compatibility of the n_T , with respect to the 2018 Planck constraints regarding the allowed range of values for n_S and tensor-to-scalar ratio r

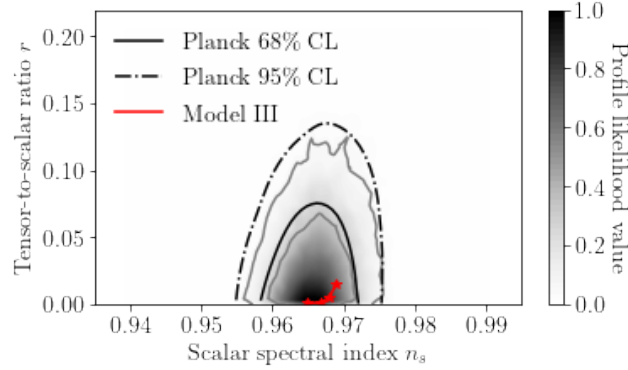


FIG. 10: The phenomenology of model III confronted with the Planck 2018 likelihood curves for various optimal values of the free parameters.

the qualitative analysis of the slow-roll parameters that derive from this potential,

$$V(\phi) = \frac{1}{k^4} \left[1 + \cos\left(\frac{\phi}{f}\right) \right] \quad (74)$$

in which case the parameter f , with $[f] = [m]$ represents the a-priori unknown, symmetry breaking scale. With that in mind, we make use of Eq. (25) to derive the non-minimally coupling function to the theory,

$$\xi(\phi) = \frac{3b^2}{4 \left(\cos\left(\frac{\phi}{f}\right) + \gamma k^4 + 1 \right)} \quad (75)$$

where the introduction of the $\gamma > 0$ term stems from the need to avoid divergences in the coupling function. After computing the slow-roll indices for this coupling function we get,

$$\epsilon_1 \simeq \frac{f^2 \kappa^2 \sin^2\left(\frac{\phi}{f}\right)}{2\beta \left(\cos\left(\frac{\phi}{f}\right) - 2\right)^2} \quad (76)$$

$$\epsilon_2 \simeq \frac{-4\beta - f^2 \kappa^2 + 8\beta \cos\left(\frac{\phi}{f}\right) + f^2 \kappa^2 \cos\left(\frac{2\phi}{f}\right)}{4\beta \left(-2 + \cos\left(\frac{\phi}{f}\right)\right)^2} \quad (77)$$

$$\epsilon_3 \simeq 0 \quad (78)$$

$$(79)$$

$$\epsilon_4 \simeq \frac{3\beta \left[-9 + 4 \cos\left(\frac{\phi}{f}\right) + \cos\left(\frac{2\phi}{f}\right)\right] \sin^2\left(\frac{\phi}{2f}\right)}{\left(-2 + \cos\left(\frac{\phi}{f}\right)\right) \left(15\beta + 4f^2 \kappa^2 + (-18\beta + 4f^2 \kappa^2) \cos\left(\frac{\phi}{f}\right) + 3\beta \cos\left(\frac{2\phi}{f}\right)\right)} \quad (80)$$

$$\epsilon_5 \simeq -\sin^2\left(\frac{\phi}{2f}\right) \quad (81)$$

$$\epsilon_6 \simeq -\frac{\sin^2\left(\frac{\phi}{f}\right)}{2 \left(\cos\left(\frac{\phi}{f}\right) - 2\right)^2} \quad (82)$$

all of which constitute well-defined functions with no irregularities in their expressions, a feature that will prove invaluable later on. Having obtained the functional forms of the slow-roll indices, the end of inflation is easily obtained if one considers $\epsilon_1(\phi_f) = 1$. This poses a transcendental equation that has no algebraic solution, but given that in the Planckian scale the ratio $x = \frac{\phi}{f}$

1 it is permissible to express the first slow-roll index with its leading order in its respective Taylor series expansion, yielding,

$$\epsilon_1(\phi) \simeq \frac{\kappa^2 \phi^2}{2\beta} - \frac{2\kappa^2 \phi^4}{3\beta f^2} + \mathcal{O}(\phi)^6 \quad (83)$$

the resulting solutions upon substituting the approximated functional form become,

$$\phi_f = \pm \sqrt{\frac{\sqrt{3}f \sqrt{3f^2 \kappa^4 - 32\beta \kappa^2}}{8\kappa^2} + \frac{3f^2}{8}} \quad \text{or} \quad \pm \frac{\sqrt{3f^2 - \frac{\sqrt{3}f \sqrt{\kappa^2(-32\beta + 3f^2 \kappa^2)}}{\kappa^2}}}{2\sqrt{2}} \quad (84)$$

meanwhile, the value of the field at the first horizon crossing will be made following a simple expansion of ξ' around $\phi = 0$,

$$\xi'(\phi) = \frac{3\beta^2 \phi}{8f^2} + \mathcal{O}(x^3) \quad (85)$$

where obviously even powers of x vanish in the series as the derivative of the scalar coupling function, being an even function itself, will be odd overall. This leads to a value of the scalar field at the first horizon crossing that reads,

$$\phi_i = \frac{\sqrt{2\beta}}{e^N \kappa} \quad (86)$$

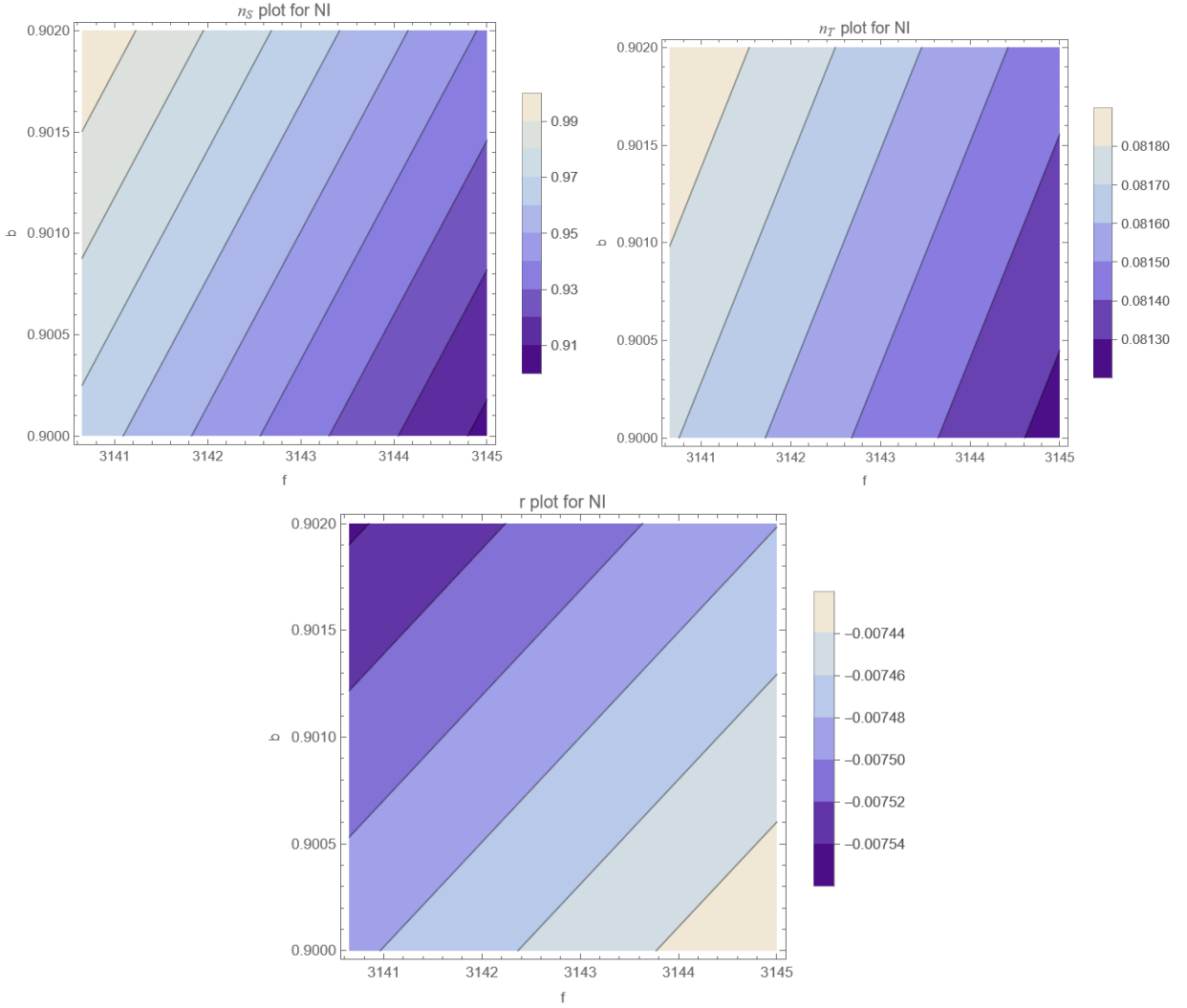


FIG. 11: The qualitative and quantitative trends of the spectral indices of primordial perturbations, for a range of values within the margins of 2018 Planck compatibility and, possibly, blue-tilt of n_T .

with $N = 60$ being the number of e-folds at the end of inflation. Substituting into the spectral indices we immediately observe that $r \rightarrow 0$, since it is on the scale of 10^{-40} safely within the margins of the Planck observational data. These approximations have been handled with extreme diligence to ensure the qualitative behavior of the spectral indices. In hindsight, one could obtain very similar final results by considering even lower leading-order Taylor series due to the great convergence satisfied by the Planckian values of the a-priori unknown scale f . Finally, the graphs of Fig. (11) encapsulate all there is to know about the spectral indices at the first horizon crossing, The plots of Fig. 11 portray the qualitative and quantitative trends of the spectral indices of primordial perturbations, for a range of values within the margins of 2018 Planck compatibility and, possibly, blue-tilt of n_T . It is important to note that the values of the tensor-to-scalar ratio of the perturbation's amplitudes have been rescaled as $r' \rightarrow 10^{14}r$ in order to display its features in a palpable fashion, whereas the values of the symmetry breaking scales are of the order of 10^{18} GeV. Thereby affirming the Planckian permission of observational-constraint-respecting inflation and hinting at a possible blue tilt of the tensor spectral index. Also, it is to be noted that the tensor-to-scalar ratio pertains to values whose magnitude respects the 2018 Planck constraints imposing $r < 0.064$ and in addition the BICEP/Keck constraints [66] are respected too. Lastly, we will concern ourselves with the validity of the slow-roll approximations for selected sets of blue-tilt satisfying values of the free parameters (f, β) . Our results for viable cases listed in Table VI, are accompanied by the validity of the approximations which are estimated in orders of magnitude as seen in Table VII. Therefore, all of our data sets that satisfy the 2018 Planck constraints are also well approximated within what is permissible from the slow-roll conditions. In addition, in Fig. 12 we confront model IV with the Planck 2018 likelihood curves, again for various suitably chosen values of the free parameters. As it can be seen in this case too,

	$f(10^{18} GeV)$	β	n_S	$n_T(10^{-30})$	$r(10^{-18})$
Set 1)	3141	0.905	0.966	8.2	7.65
Set 2)	3142	0.91	0.962	8.24	7.75
Set 3)	3143	0.9105	0.967	8.5	7.89
Set 4)	3144	0.93	0.966	9.13	8.08

TABLE VI: Viable Scenarios for Natural inflation.

	$f(10^{18} GeV)$	β	ϵ_1	$\frac{\dot{\phi}^2}{2V}$	ϵ_2	$\kappa \frac{\xi'}{\xi''}$	$\frac{4\kappa^4 \xi'^2 V}{3\beta^2 \xi''}$
Set 1)	3141	0.905	$\mathcal{O}(10^{-80})$	$\mathcal{O}(10^{-84})$	$\mathcal{O}(10^{-1})$	$\mathcal{O}(10^{-34})$	$\mathcal{O}(10^{-53})$
Set 2)	3142	0.91	$\mathcal{O}(10^{-80})$	$\mathcal{O}(10^{-84})$	$\mathcal{O}(10^{-1})$	$\mathcal{O}(10^{-34})$	$\mathcal{O}(10^{-53})$
Set 3)	3143	0.9105	$\mathcal{O}(10^{-80})$	$\mathcal{O}(10^{-84})$	$\mathcal{O}(10^{-1})$	$\mathcal{O}(10^{-31})$	$\mathcal{O}(10^{-53})$
Set 4)	3144	0.93	$\mathcal{O}(10^{-80})$	$\mathcal{O}(10^{-84})$	$\mathcal{O}(10^{-1})$	$\mathcal{O}(10^{-34})$	$\mathcal{O}(10^{-53})$

TABLE VII: Validity of the slow-roll approximations for the Natural inflation scenario. Notice how only one case scenario does not meet the necessary prerequisites.

the model is nicely fitted in the sweet spot of the Planck likelihood curves.

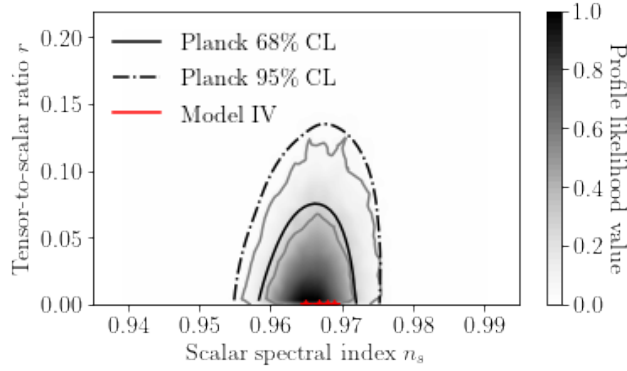


FIG. 12: The phenomenology of model IV confronted with the Planck 2018 likelihood curves for various optimal values of the free parameters.

E. Model V: Logarithmic Potential Inflation model for $V(\phi)$ (LPI)

In this case we consider the potential of Logarithmic Potential Inflation (LPI) theory, namely,

$$V(\phi) = M^4 \left(\frac{\phi}{\phi_0} \right)^p \left(\ln \frac{\phi}{\phi_0} \right)^q \quad (87)$$

The choices $(p = 4, q = 1)$, $(p = 1, q = 2)$, $(p = 4, q = 3)$ match different Yang-Mills composite models. In the LPI models M and ϕ_0 are related to a mass scale of the underlying theory, similarly here, ϕ_0 sets the scale at which inflation can occur and is permitted to take either super-Planckian or sub-Planckian values. The parameter p is not bounded to any restrictions, while the parameter q has to be an integer (and in some cases, an even integer) to ensure a well-defined potential. Solving Eq. (25), we find the coupling function to be,

$$\xi(\phi) = \frac{3 \left(\frac{\phi}{\phi_0} \right)^{-P} \ln \left(\frac{\phi}{\phi_0} \right)^{-q}}{4M^4 \kappa^4 \beta^2} \quad (88)$$

and thus, we can proceed to the slow-roll analysis of the potential.

If, for convenience, we set $\frac{\phi}{\phi_0} = x$, $p(p+1) = P$, $q(q+1) = Q$, the slow-roll indices for the LPI scenario can take the form,

$$\epsilon_1 \simeq \frac{\kappa^2 \phi^2}{2\beta} \frac{\log(x)^2 (q + p \log(x))^2}{(Q + \log(x)(q + 2pq + P \log(x)))} \quad (89)$$

$$\epsilon_2 \simeq -\frac{qQ + a_1 \ln(x) + a_2 \ln^2(x) + a_3 \ln^3(x) + a_4 \ln^4(x)}{(Q + (2p+1)q \ln(x) + P \ln^2(x))^2} \quad (90)$$

$$\epsilon_3 \simeq 0 \quad (91)$$

$$\epsilon_5 \simeq -\frac{(p \ln(x) + q)^2}{2\beta^4 (\log(x)) ((2p+1)q + P \log(x) + Q)} \quad (92)$$

$$\epsilon_6 \simeq -\frac{(q + p \ln(x))^2 Q^2 + b_1 \ln(x) + b_2 \ln(x)^2 + b_3 \ln(x)^3 + b_4 \ln(x)^4}{2\beta^4 (Q + q(1 + 2p) \ln(x) + P \ln(x)^2)^3} \quad (93)$$

$$(94)$$

where a_i and b_i are functions of p and q , that are defined as follows,

$$\begin{aligned} a_1 &= Q(2p + q) \\ a_2 &= P + q \left(3p + 1 + \frac{\kappa^2 \phi^2}{2\beta} \right) \\ a_3 &= 2qp \left(\frac{3p}{2} + 1 + \frac{\kappa^2 \phi^2}{2\beta} \right) \\ a_4 &= p \left(P + p \frac{\kappa^2 \phi^2}{2\beta} \right) \end{aligned}$$

$$\begin{aligned} b_1 &= 2Qq(1 + 2p) \\ b_2 &= q \left(2P(1 + 3q) + q \left(1 - \frac{\kappa^2 \phi^2}{2\beta} \right) \right) \\ b_3 &= 2q \left(P(1 + 2p) - \frac{\kappa^2 \phi^2}{2\beta} \right) \\ b_4 &= P^2 - \frac{\kappa^2 \phi^2}{2\beta} \end{aligned}$$

The slow-roll index ϵ_4 has a rather complicated expression and is not included as it extends to the 6th order in $\ln(x)$, with higher complexity in the coefficients. Using the Eqs. (40-42) we can proceed to the scalar spectral index n_S , the tensor spectral index n_T and the tensor-to-spectral ratio r . If we further define $Q_p = q(1 + 2p)$, $Q_\beta = \frac{q^2}{2} + Q\beta^4$ and $P_\beta = \frac{p^2}{2} + P\beta^4$, we can write:

$$n_S = 1 - 4\epsilon_1 - 2\epsilon_2 - 2\epsilon_4 \quad (95)$$

$$n_T = \frac{(q + p \ln(x))^2 Q^2 + 2c_1 \ln(x) + c_2 \ln(x)^2 + 2c_3 \ln(x)^3 + c_4 \ln(x)^4}{\beta^4 (Q + Q_p \ln(x) + P \ln(x)^2)^3} \quad (96)$$

$$r = 16\epsilon_1 \quad (97)$$

	p	q	$\phi_0(10^{18} GeV)$	β	n_S	n_T	r
set 1	0.1	6	5×10^9	0.6	0.964	0.287	1.06×10^{-66}
set 2	0.4	6	6×10^6	0.8	0.965	0.468	6.34×10^{-20}
set 3	1	6	10^6	1	0.964	0.384	0.001
set 4	1	10	3×10^4	0.95	0.965	0.447	3.9×10^{-13}
set 5	1	6	2×10^6	0.87	0.963	0.71	9.2×10^{-6}
set 6	2	10	10^5	0.9	0.964	0.91	9.2×10^{-6}
set 7	3	8	1.1×10^6	0.93	0.963	0.93	0.057

TABLE VIII: Table of viable cases for the LPI scenario.

where the extra functions c_i are described by,

$$c_1 = 2Q Q_p$$

$$c_2 = 2p q (1 + 3q) + q^2 - Q_\beta \frac{\kappa^2 \phi^2}{2\beta}$$

$$c_3 = P Q_p - (pq + \beta^4 Q_p) \frac{\kappa^2 \phi^2}{2\beta}$$

$$c_4 = P^2 - 2P_\beta \frac{\kappa^2 \phi^2}{2\beta}$$

Since n_S depends on ϵ_4 , the full expression is also not displayed for brevity. Unfortunately, due to complex form of the slow-roll parameters, the condition $\epsilon_1 = 1$ at the end of inflation and Eqs. (44) cannot be solved analytically, the field at the first horizon crossing, ϕ_i , and at the end of inflation, ϕ_f , have been computed numerically. As usual, 60 e -foldings have been assumed to occur between the two events. No further simplifications or assumptions have been used. The Table VIII presents 4 sets that respect the Planck data and demonstrates that it is possible to achieve a tensor spectral index as high as, $n_T = 0.9$, in three cases, namely sets 5-7. Two regions are distinguished, $0 \lesssim n_T \lesssim 0.45$ and $0.7 \lesssim n_T \lesssim 1$, but the analysis holds the same, as the behavior of the indices is similar. In most cases, $q = 6$ was a crucial choice, as it made it possible for the spectral indices to acquire meaningful values, but $q = 8$ and $q = 10$ also proved to work. The region $0 < p \leq 1$ was most suitable in order to keep a low r and a sensible tensor blue-tilt, $0.2 \lesssim n_T \lesssim 0.45$, while $p = 2$ and $p = 3$ where most suitable. For lower n_T and while $0 < p < 1$, the tensor-to-scalar ratio is significantly lower (respecting the Planck data upper limit, $r < 0.064$ and also the limit $r < 0.036$ indicated by the BICEP/Keck experiment [66], with the only case being incompatible being set 7 in Table VIII), but it exceeds this constraint at higher values of p , as it is qualitatively shown in Figs. (14) and (15).

The scale at which ϕ_0 becomes viable for our theory, at each choice of p and q , is clearly visible in the contour plots (Fig. (13)). The behavior is also similar for the sets 5,6 and 7 in the same range $[10^5 - 10^7]$. The contours seem to have weak dependence on β , but this is an illusion caused by the range scale of the parameter ϕ_0 . This is the reason an extra exemplary contour has been added (Sub-figures 16 magnified in a short interval of ϕ_0 that is in accordance to the 2018 Planck constraints. Furthermore, one can see how n_S and r evolve with the power parameter p , which strongly suggests that $p < 2$ (Figures 17(a) and 17(b)) In general, $p \geq 2$ requires $n_T > 0.5$. This model needs some care while picking the parameter q , as the indices are very sensitive to small changes in the power of the logarithm (especially comparing to the other parameters) and only discrete choices present sensible results. Lastly, in order to confirm that the analysis lies within the slow-roll regime, the initial hypotheses has to be validated, which, actually, is the case here, as depicted in the Table IX. Unfortunately, in some cases ϵ_2 is close to 0.9. Also, the approximation $r = 16\epsilon_1$ holds up to many orders. The fact that the slow-roll indices at first horizon crossing are taking such large values, makes this model phenomenologically unappealing and we need to mention this, since this model yields too large blue tilt for the tensor spectral index. Thus we cannot consider this seriously since it is a marginally correct model. In this section we considered several rescaled models of EGB gravity and one good question is when do the models yield a blue tilt in the tensor spectral index. This is of particular importance since a blue tilt might lead to detectable primordial gravitational waves as we will show in the next section. However, we need to note that the blue tilt in the tensor spectral index must be strong enough and also the model must be viable regarding the Planck data. From the models we considered, only model I and model IV yield a strong blue tilt. In general, the blue tilt in the tensor spectral index is a model dependent feature, but there is a general rule on how such a blue tilt might

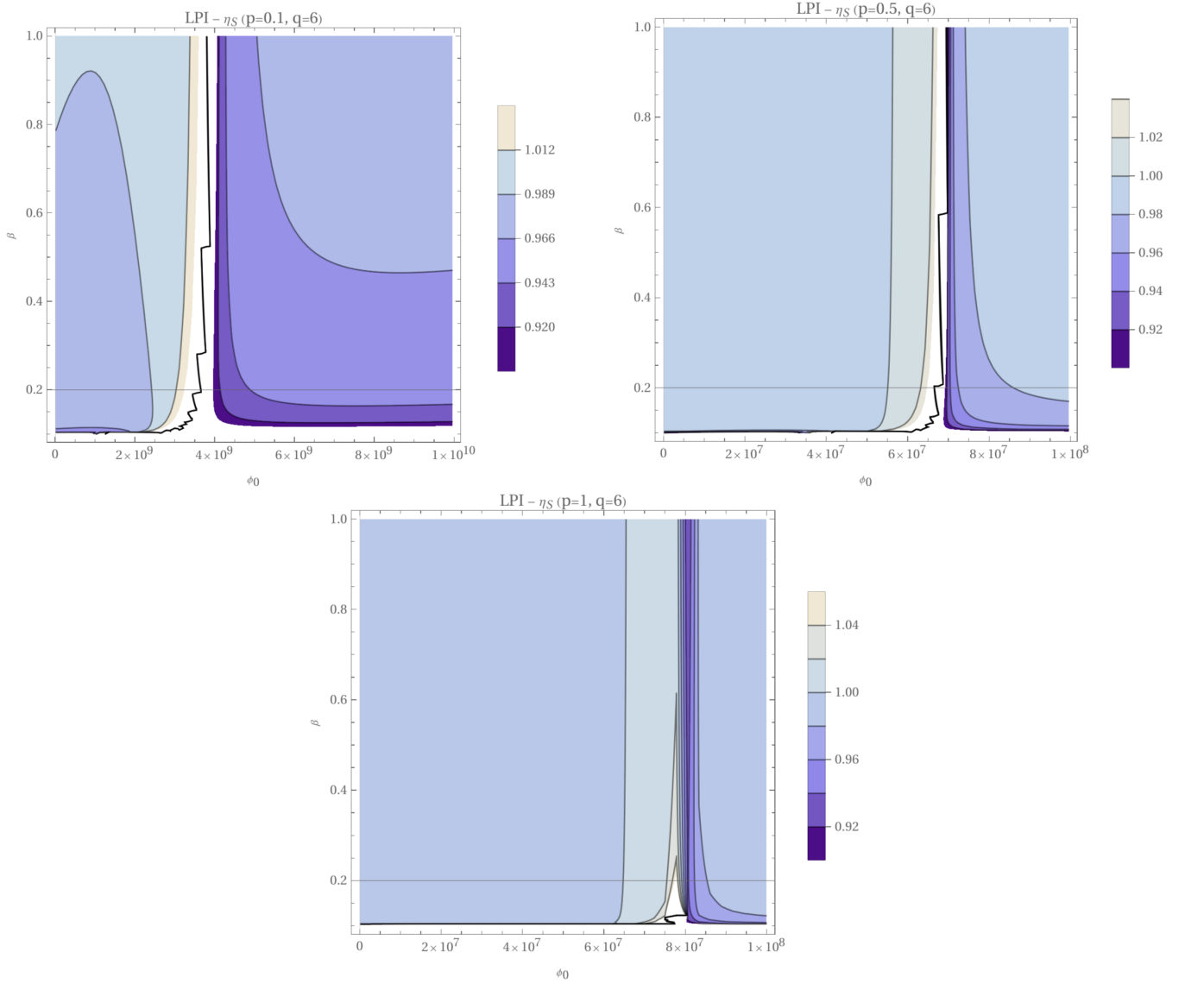


FIG. 13: The figure displays the comparison between the n_S for three different cases: (a) Contour plot of scalar spectral index for $p = 0.1$, (b) Contour plot of scalar spectral index for $p = 0.5$, and (c) Contour plot of scalar spectral index for $p = 1$. In all cases, just after the transition region where the function does not behave smoothly, the parameter ϕ_0 is on its applicable scale.

	ϵ_1	ϵ_2	ϵ_4	ϵ_6	$\kappa \frac{\xi'}{\xi''}$	$\frac{4\kappa^4 \xi'^2 V}{3\beta^2 \xi''}$
set 1	$\mathcal{O}(10^{-68})$	$\mathcal{O}(10^{-1})$	$\mathcal{O}(10^{-1})$	$\mathcal{O}(10^{-1})$	$\mathcal{O}(10^{-34})$	$\mathcal{O}(10 - 1)$
set 2	$\mathcal{O}(10^{-21})$	$\mathcal{O}(10^{-1})$	$\mathcal{O}(10^{-1})$	$\mathcal{O}(10^{-1})$	$\mathcal{O}(10^{-11})$	$\mathcal{O}(10^{-1})$
set 3	$\mathcal{O}(10^{-5})$	$\mathcal{O}(10^{-1})$	$\mathcal{O}(10^{-1})$	$\mathcal{O}(10^{-1})$	$\mathcal{O}(10^{-2})$	$\mathcal{O}(10^{-1})$
set 4	$\mathcal{O}(10^{-14})$	$\mathcal{O}(10^{-1})$	$\mathcal{O}(10^{-1})$	$\mathcal{O}(10^{-1})$	$\mathcal{O}(10^{-7})$	$\mathcal{O}(10^{-1})$
set 5	$\mathcal{O}(10^{-7})$	$\mathcal{O}(10^{-1})$	$\mathcal{O}(10^{-1})$	$\mathcal{O}(10^{-1})$	$\mathcal{O}(10^{-3})$	$\mathcal{O}(10^{-1})$
set 6	$\mathcal{O}(10^{-9})$	$\mathcal{O}(10^{-1})$	$\mathcal{O}(10^{-1})$	$\mathcal{O}(10^{-1})$	$\mathcal{O}(10^{-5})$	$\mathcal{O}(10^{-1})$
set 7	$\mathcal{O}(10^{-3})$	$\mathcal{O}(10^{-1})$	$\mathcal{O}(10^{-1})$	$\mathcal{O}(10^{-1})$	$\mathcal{O}(10^{-2})$	$\mathcal{O}(10^{-1})$

TABLE IX: Validation of the slow-roll approximations for the LPI inflation scenario.

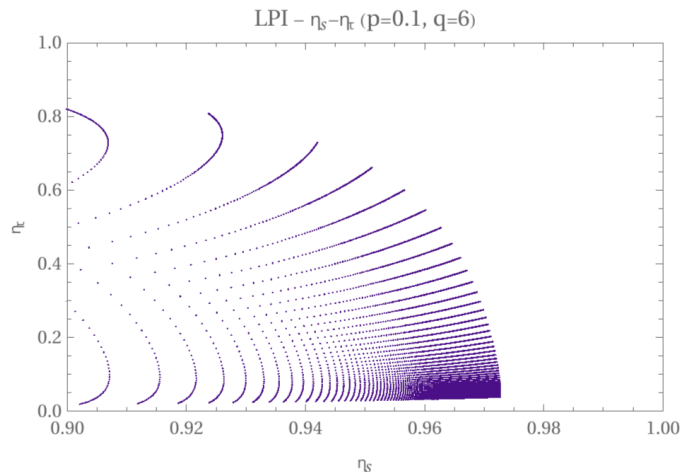


FIG. 14: List plot of $n_S - n_T$, with $p = 0.1$, portrays a dense region of points viable to the 2018 Planck data constraints with a significant blue-tilt.

occur. The method for examining this was developed in Ref. [73] and at this point we shall discuss the results in brief. Particularly, the tensor spectral index takes the form, $n_T \simeq 2 \left(-1 + \frac{1}{\lambda(\phi)} \right) \epsilon_1$ at leading order, where $\lambda(\phi)$ is defined in Eq. (36) and recall that it also contains the rescaling parameter β . As it was shown in [73], the blue tilted tensor spectral index is obtained whenever $\xi''(\phi_*)V(\phi_*) > 0$ at first horizon crossing. So model building may be used in such a way so that the constraint $\xi''(\phi_*)V(\phi_*) > 0$ is satisfied at first horizon crossing, and simultaneously the model must be compatible with the Planck and BICEP/Keck data. Furthermore, in Fig. 18 we confront model II with the Planck 2018 likelihood curves for various suitably chosen values of the free parameters. As it can be seen, the model is nicely fitted in the Planck likelihood curves and for some values of the free parameters, the model is phenomenologically fitted in the sweet spot of the Planck data.

IV. PRIMORDIAL GRAVITATIONAL WAVE ENERGY SPECTRUM FOR RESCALED EGB THEORIES

In the previous sections we developed the theoretical framework of rescaled EGB gravity, and we studied several models of interest which were viable phenomenologically. More importantly, some of these yielded a blue-tilted tensor spectrum, while being simultaneously compatible with the Planck constraints on the scalar spectral index of primordial perturbations and the tensor-to-scalar ratio. In this section we shall investigate whether some of these models can yield a detectable signal of primordial gravitational waves, so we shall calculate the energy spectrum of the primordial gravitational waves for the models of interest. In the literature there is a large stream of articles studying the primordial gravitational waves, see for example In the literature there exist many works which consider theoretical predictions on primordial gravitational waves, for a mainstream of articles see for example Refs. [61, 62, 67, 74–114, 114]. The models which are interesting phenomenologically, are the power law model of Eq. (44) in which case, the tensor spectral index takes the value $n_T = 0.56$ and also $r = 0.02$ for the set 2 appearing in Table I. Also, another model we shall consider is the logarithmic model of inflation (87) and specifically the set 6 from Table VIII, which yields $n_T = 0.91$ and $r = 9.2 \times 10^{-6}$, however this model has to be treated with caution since the approximations marginally hold true. The energy spectrum today of an inflationary theory is,

$$\Omega_{\text{gw}}(f) = \frac{k^2}{12H_0^2} \Delta_h^2(k), \quad (98)$$

with $\Delta_h^2(k)$ defined as,

$$\Delta_h^2(k) = \Delta_h^{(p)}(k)^2 \left(\frac{\Omega_m}{\Omega_\Lambda} \right)^2 \left(\frac{g_*(T_{\text{in}})}{g_{*0}} \right) \left(\frac{g_{*s0}}{g_{*s}(T_{\text{in}})} \right)^{4/3} \left(\frac{3j_1(k\tau_0)}{k\tau_0} \right)^2 T_1^2(x_{\text{eq}}) T_2^2(x_R),$$

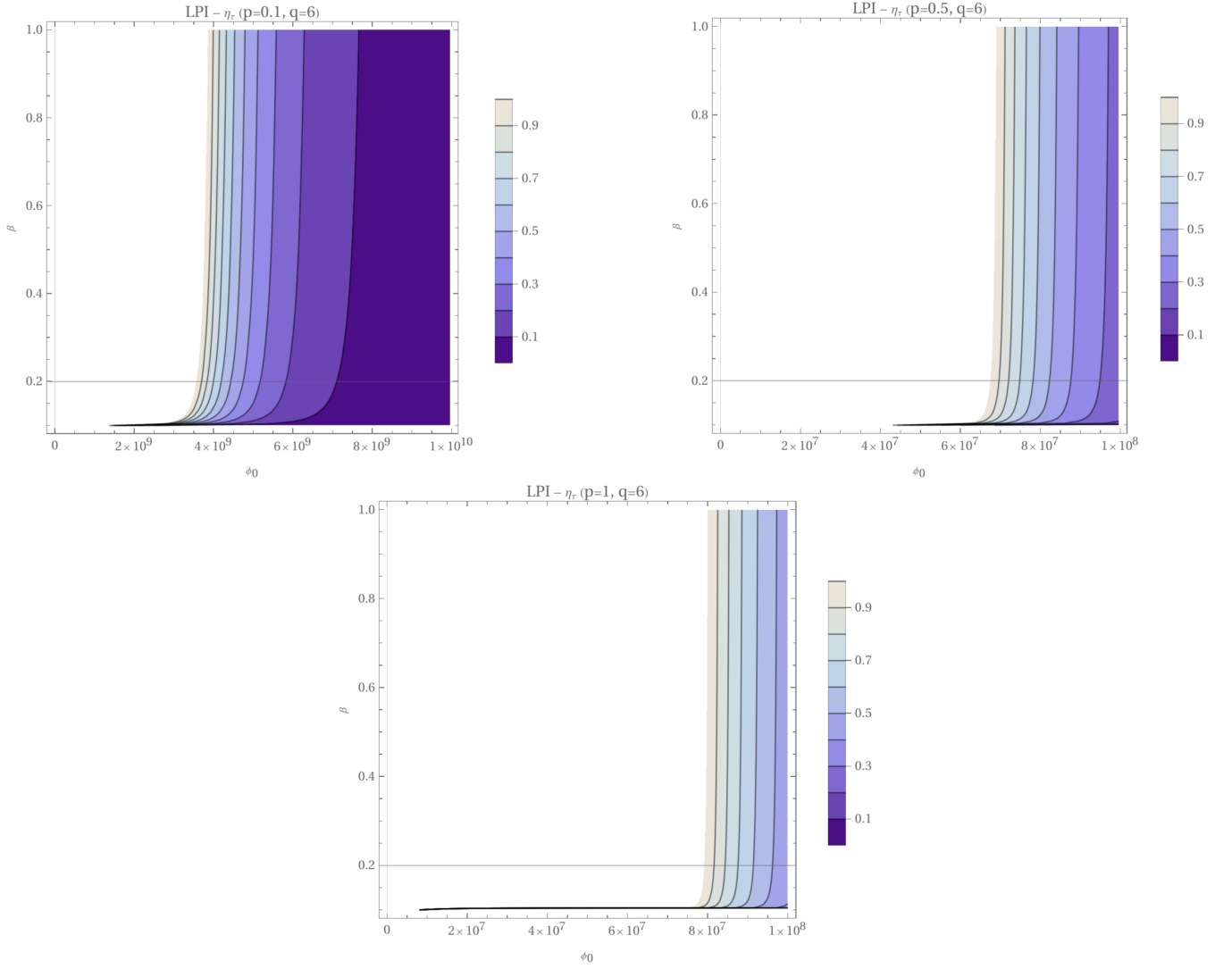


FIG. 15: This figure displays a comparison between the n_T contours for three different cases: (a) Contour plot of tensor spectral index for $p = 0.1$, (b) Contour plot of tensor spectral index for $p = 0.5$, and (c) Contour plot of tensor spectral index for $p = 1$. Notice how n_T becomes relevant to our range after the anomalous region, which is visible in n_S contours.

while $\Delta_h^{(p)}(k)^2$ stands for the inflationary tensor power spectrum, which is defined as,

$$\Delta_h^{(p)}(k)^2 = \mathcal{A}_T(k_{ref}) \left(\frac{k}{k_{ref}} \right)^{n_T}. \quad (99)$$

We evaluate the inflationary tensor power spectrum at the CMB pivot scale $k_{ref} = 0.002 \text{ Mpc}^{-1}$ and n_T denotes the spectral index of the tensor perturbations, while $\mathcal{A}_T(k_{ref})$ stands for the amplitude of the tensor perturbations, which is,

$$\mathcal{A}_T(k_{ref}) = r \mathcal{P}_\zeta(k_{ref}). \quad (100)$$

Also r is the tensor-to-scalar ratio and $\mathcal{P}_\zeta(k_{ref})$ denotes the amplitude of the primordial scalar perturbations. Therefore, we have,

$$\Delta_h^{(p)}(k)^2 = r \mathcal{P}_\zeta(k_{ref}) \left(\frac{k}{k_{ref}} \right)^{n_T}, \quad (101)$$

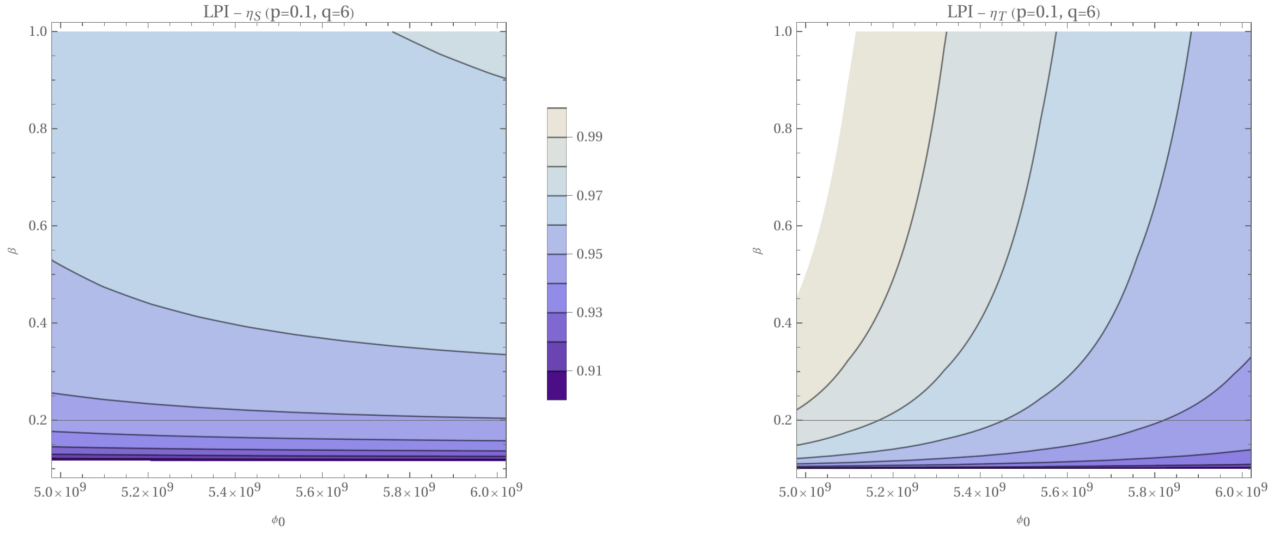


FIG. 16: This figure displays the contour plots of (a) Scalar spectral index n_S and (b) Tensor spectral index n_T with ϕ_0 restricted to the region of interest, for the case $p = 0.1$. The remaining plots are similar.

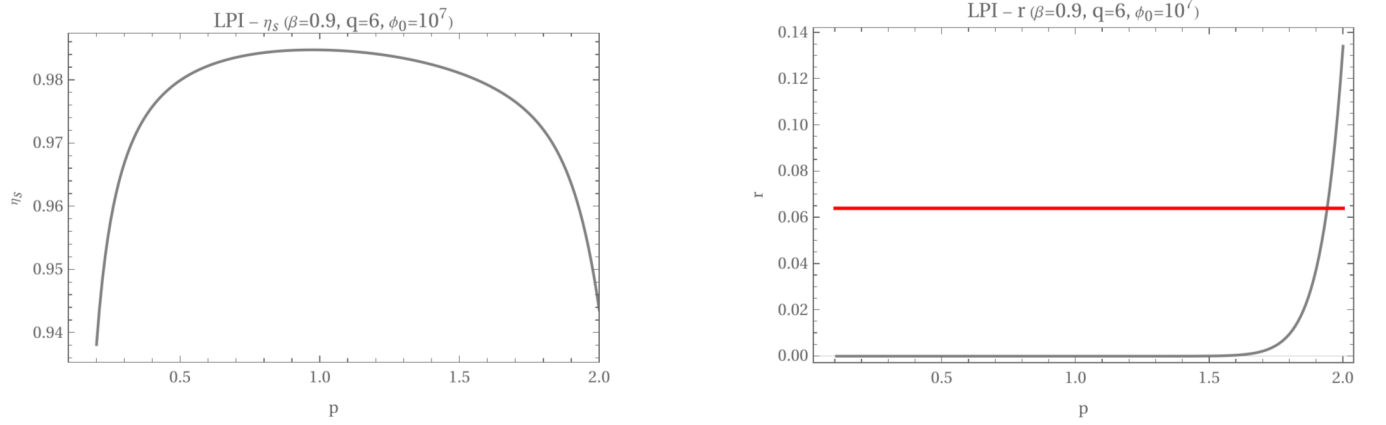


FIG. 17: The figure shows two plots for $q = 6$, $\phi_0 = 10^7$ and $\beta = 0.9$: (a) Plot of the scalar spectral index n_S as it changes with p , and (b) Plot of the tensor-to-scalar ratio r as it changes with p , with the red line denoting the Planck constraint $r < 0.064$.

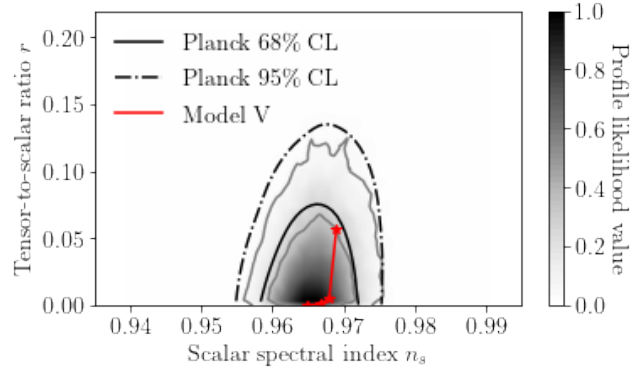


FIG. 18: The phenomenology of model V confronted with the Planck 2018 likelihood curves for various optimal values of the free parameters.

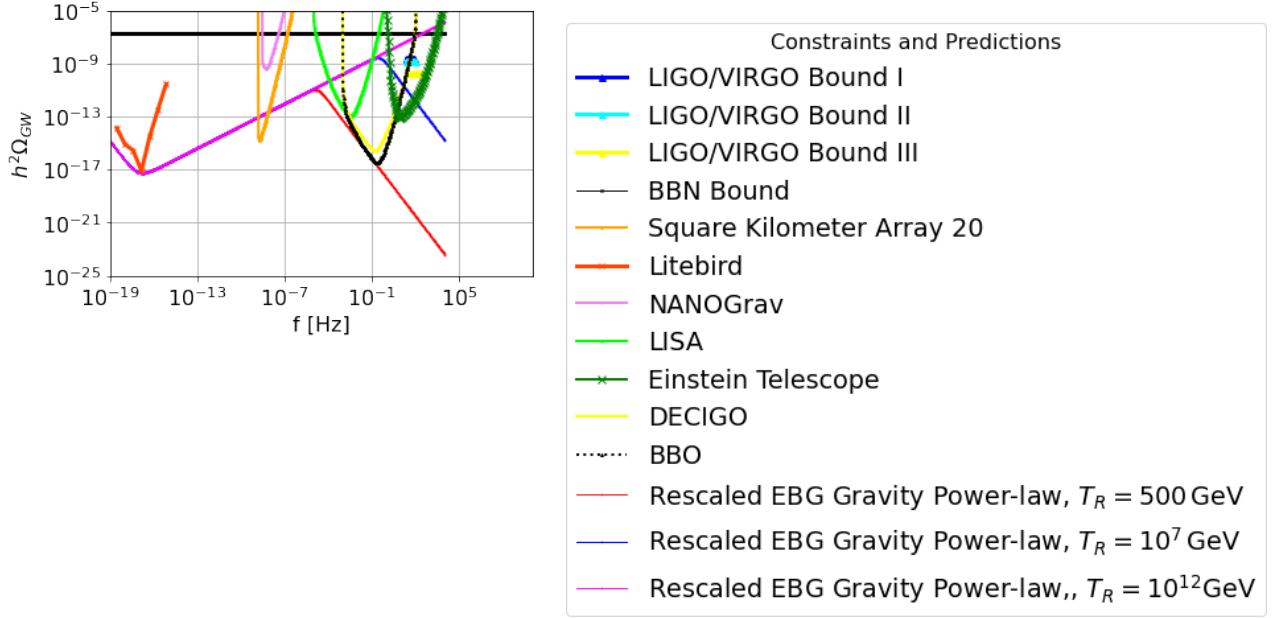


FIG. 19: The h^2 -scaled gravitational wave energy spectrum for the rescaled EBG power-law model of gravity (44) for three distinct reheating temperatures, $T_R = 5 \times 10^2 \text{ GeV}$, $T_R = 10^7 \text{ GeV}$ and $T_R = 10^{12} \text{ GeV}$.

hence the energy spectrum of the primordial gravitational waves which we shall calculate for the rescaled EBG theories reads,

$$\Omega_{\text{gw}}(f) = \frac{k^2}{12H_0^2} r \mathcal{P}_\zeta(k_{\text{ref}}) \left(\frac{k}{k_{\text{ref}}} \right)^{n\tau} \left(\frac{\Omega_m}{\Omega_\Lambda} \right)^2 \left(\frac{g_*(T_{\text{in}})}{g_{*0}} \right) \left(\frac{g_{*s0}}{g_{*s}(T_{\text{in}})} \right)^{4/3} \left(\frac{3j_1(k\tau_0)}{k\tau_0} \right)^2 T_1^2(x_{\text{eq}}) T_2^2(x_R),$$

where T_{in} denotes the horizon reentry temperature,

$$T_{\text{in}} \simeq 5.8 \times 10^6 \text{ GeV} \left(\frac{g_{*s}(T_{\text{in}})}{106.75} \right)^{-1/6} \left(\frac{k}{10^{14} \text{ Mpc}^{-1}} \right), \quad (102)$$

and also the transfer function $T_1(x_{\text{eq}})$ is defined to be equal to,

$$T_1^2(x_{\text{eq}}) = [1 + 1.57x_{\text{eq}} + 3.42x_{\text{eq}}^2], \quad (103)$$

where $x_{\text{eq}} = k/k_{\text{eq}}$ and $k_{\text{eq}} \equiv a(t_{\text{eq}})H(t_{\text{eq}}) = 7.1 \times 10^{-2} \Omega_m h^2 \text{ Mpc}^{-1}$, and in addition the transfer function $T_2(x_R)$ is equal to,

$$T_2^2(x_R) = (1 - 0.22x^{1.5} + 0.65x^2)^{-1}, \quad (104)$$

with $x_R = \frac{k}{k_R}$, and in addition the wavenumber at the epoch of maximum reheating is,

$$k_R \simeq 1.7 \times 10^{13} \text{ Mpc}^{-1} \left(\frac{g_{*s}(T_R)}{106.75} \right)^{1/6} \left(\frac{T_R}{10^6 \text{ GeV}} \right), \quad (105)$$

where T_R denotes the reheating temperature, which is very important in our consideration, and we shall discuss its values later on in this section. Also, $g_*(T_{\text{in}}(k))$ is defined as,

$$g_*(T_{\text{in}}(k)) = g_{*0} \left(\frac{A + \tanh \left[-2.5 \log_{10} \left(\frac{k/2\pi}{2.5 \times 10^{-12} \text{ Hz}} \right) \right]}{A + 1} \right) \left(\frac{B + \tanh \left[-2 \log_{10} \left(\frac{k/2\pi}{6 \times 10^{-19} \text{ Hz}} \right) \right]}{B + 1} \right), \quad (106)$$

where A and B parameters are equal to,

$$A = \frac{-1 - 10.75/g_{*0}}{-1 + 10.75g_{*0}}, \quad (107)$$

$$B = \frac{-1 - g_{max}/10.75}{-1 + g_{max}/10.75}, \quad (108)$$

with $g_{max} = 106.75$ and $g_{*0} = 3.36$. Furthermore, $g_{*0}(T_{in}(k))$ can be evaluated by using Eqs. (106), (107) and (108), by replacing $g_{*0} = 3.36$ with $g_{*s} = 3.91$. Now let us proceed by evaluating the h^2 -scaled energy spectrum

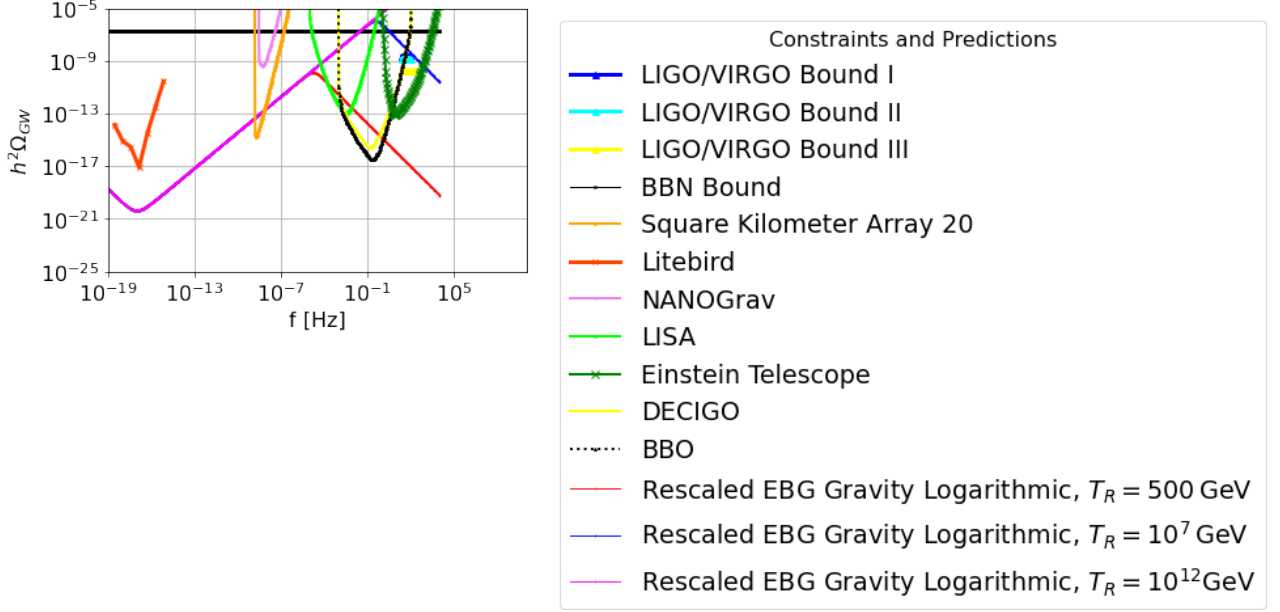


FIG. 20: The h^2 -scaled gravitational wave energy spectrum for the rescaled EBG logarithmic model of gravity (87) for three distinct reheating temperatures, $T_R = 5 \times 10^2 \text{ GeV}$, $T_R = 10^7 \text{ GeV}$ and $T_R = 10^{12} \text{ GeV}$.

of the primordial gravitational waves for the rescaled EBG models we mentioned earlier, namely the power law model of Eq. (44) and the logarithmic model (87). We shall consider three reheating temperatures, namely a high reheating temperature $T_R = 10^{12} \text{ GeV}$, an intermediate one with $T_R = 10^7 \text{ GeV}$ and a low reheating temperature $T_R = 5 \times 10^2 \text{ GeV}$. In Fig. 19 we present the predicted h^2 -scaled energy spectrum of the primordial gravitational waves for the power-law model (44) for $n_{\mathcal{T}} = 0.56$ and also $r = 0.02$, while in Fig. 20 we present the predicted h^2 -scaled energy spectrum of the primordial gravitational waves for the logarithmic model (44) for $n_{\mathcal{T}} = 0.91$ and $r = 9.2 \times 10^{-6}$. As it can be seen, the power-law model leads to a detectable signal which can be detected by the SKA, LISA, BBO, DECIGO and the Einstein Telescope, for intermediate reheating temperatures. The high reheating temperature scenario is excluded by the LIGO constraints, while the low-reheating temperature scenario can be detectable only by the SKA experiment. Regarding the logarithmic model, only the low-reheating temperature scenario may be detectable, while the high and intermediate reheating temperature scenarios are excluded by the current LIGO constraints. In this scenario, the low-reheating case can be detectable by LISA, SKA, BBO and DECIGO. Thus the phenomenology of rescaled EBG gravity is quite promising and can lead to particularly interesting results which may be verified by future gravitational wave experiments.

V. CONCLUDING REMARKS

In this work, we employed a self-consistent and simplified rescaled EBG inflationary theoretical framework, and we analyzed several models of theoretical interest. We developed the formalism of the rescaled EBG theories of gravity, and we demonstrated how the rescaled theory can directly affect the primordial scalar and tensor perturbations. Accordingly, we showed how the slow-roll indices will be affected and eventually how the inflationary observational

indices are changed. We applied the formalism for specifically chosen models and we showed how these models can provide a viable inflationary phenomenology. Specifically, the most important models that we analyzed are the natural inflation potential extended in an EGB theory, and a power-law scalar potential. As we demonstrated, the rescaled versions of these models can provide a viable inflationary theory, compatible with the latest Planck data and more importantly these models can lead to a significantly blue-tilted tensor spectral index, a feature that is phenomenologically appealing since blue-tilted inflationary theories can lead to a detectable signal of primordial gravitational waves. We calculated the energy spectrum of the primordial gravitational waves for the models of interest and we showed that, depending on the reheating temperature, these models can lead to detectable stochastic signals in the future gravitational wave detectors, and specifically some signals can be detected by LISA, SKA, BBO, DECIGO and the Einstein Telescope. What we did not consider is the dark energy implications of this rescaled EGB theories. Basically, the rescaled EGB theories contain a non-trivial $F(R)$ gravity part, which primordially contributes only the rescaling of the Einstein-Hilbert term, but at late times it can become significant since the curvature is not large anymore. Thus, phenomena like the ones described in Ref. [64] might occur, in the presence of a non-trivial Gauss-Bonnet coupling in the inflaton. This is of particular importance since the $F(R)$ gravity part may significantly affect the late-time evolution of the EGB theory. In this paper we considered a non-trivial part for the $F(R)$ gravity of exponential form $e^{-\Lambda/R}$ which can easily dominate the late-time evolution. On the contrary, primordially this exponential term contributes nothing more than a rescaling in the Einstein-Hilbert term, which affects the EGB phenomenology at the first horizon crossing. The rescaling of the Einstein-Hilbert term becomes negligible near the end of inflation, after the Universe has expanded significantly and the Ricci scalar basically takes small values. Hence the rescaling only occurs near the first horizon crossing and does not occur during the subsequent evolution eras of our Universe, from the end of inflation, and after, including the reheating and radiation era and thereafter. Such rescaling theories can be considered in the context of other modified gravities, like for example $f(R, T)$ or $F(R, G)$, in the latter theories however the problems of ghosts must be considered. In the present context ghosts are not a problem because the theory is an $F(R)$ gravity extension of the standard EGB theory, which is known to be ghost free in the linear perturbations of the metric context. In addition, one may consider such rescaled $F(R)$ theories in strong gravity regimes, such as near black holes or in neutron stars. We have not considered these effects here, but it certainly would be interesting to address such problems in a study focused on compact objects with extreme gravity.

Before closing this article, we need to discuss an important issue related with the duration of the reheating era. As it was demonstrated in Ref. [115], the equation of state (EoS) of the Universe at the post-inflationary era may affect the energy spectrum of the primordial gravitational waves in a direct way. As it is discussed in [115], the transition from inflation to an intermediate EoS Universe, before the Universe enters its radiation domination EoS $w = 1/3$, can have an imprint in the form of a peak on the energy spectrum of the primordial gravitational waves. This important aspect was not taken into account in this work, but we aim to discuss this issue soon in the context of both $F(R)$ gravity and EGB gravity. Note that the transition from an inflationary de Sitter epoch to the radiation domination era in the context of simple EGB theories, was studied in Ref. [116], so these considerations must also be taken into account when considering the duration and total background EoS in the context of EGB theories.

Acknowledgments

This research has been is funded by the Committee of Science of the Ministry of Education and Science of the Republic of Kazakhstan (Grant No. AP19674478).

-
- [1] A. D. Linde, Lect. Notes Phys. **738** (2008) 1 [arXiv:0705.0164 [hep-th]].
 - [2] D. S. Gorbunov and V. A. Rubakov, “Introduction to the theory of the early universe: Cosmological perturbations and inflationary theory,” Hackensack, USA: World Scientific (2011) 489 p;
 - [3] A. Linde, arXiv:1402.0526 [hep-th];
 - [4] D. H. Lyth and A. Riotto, Phys. Rept. **314** (1999) 1 [hep-ph/9807278].
 - [5] M. H. Abitbol *et al.* [Simons Observatory], Bull. Am. Astron. Soc. **51** (2019), 147 [arXiv:1907.08284 [astro-ph.IM]].
 - [6] K. N. Abazajian *et al.* [CMB-S4], [arXiv:1610.02743 [astro-ph.CO]].
 - [7] S. Hild, M. Abernathy, F. Acernese, P. Amaro-Seoane, N. Andersson, K. Arun, F. Barone, B. Barr, M. Barsuglia and M. Beker, *et al.* Class. Quant. Grav. **28** (2011), 094013 doi:10.1088/0264-9381/28/9/094013 [arXiv:1012.0908 [gr-qc]].
 - [8] J. Baker, J. Bellovary, P. L. Bender, E. Berti, R. Caldwell, J. Camp, J. W. Conklin, N. Cornish, C. Cutler and R. DeRosa, *et al.* [arXiv:1907.06482 [astro-ph.IM]].
 - [9] T. L. Smith and R. Caldwell, Phys. Rev. D **100** (2019) no.10, 104055 doi:10.1103/PhysRevD.100.104055 [arXiv:1908.00546 [astro-ph.CO]].

- [10] J. Crowder and N. J. Cornish, Phys. Rev. D **72** (2005), 083005 doi:10.1103/PhysRevD.72.083005 [arXiv:gr-qc/0506015 [gr-qc]].
- [11] T. L. Smith and R. Caldwell, Phys. Rev. D **95** (2017) no.4, 044036 doi:10.1103/PhysRevD.95.044036 [arXiv:1609.05901 [gr-qc]].
- [12] N. Seto, S. Kawamura and T. Nakamura, Phys. Rev. Lett. **87** (2001), 221103 doi:10.1103/PhysRevLett.87.221103 [arXiv:astro-ph/0108011 [astro-ph]].
- [13] S. Kawamura, M. Ando, N. Seto, S. Sato, M. Musha, I. Kawano, J. Yokoyama, T. Tanaka, K. Ioka and T. Akutsu, *et al.* [arXiv:2006.13545 [gr-qc]].
- [14] A. Weltman, P. Bull, S. Camera, K. Kelley, H. Padmanabhan, J. Pritchard, A. Raccanelli, S. Riemer-Sørensen, L. Shao and S. Andrianomena, *et al.* Publ. Astron. Soc. Austral. **37** (2020), e002 doi:10.1017/pasa.2019.42 [arXiv:1810.02680 [astro-ph.CO]].
- [15] P. Auclair *et al.* [LISA Cosmology Working Group], [arXiv:2204.05434 [astro-ph.CO]].
- [16] G. Agazie *et al.* [NANOGrav], Astrophys. J. Lett. **951** (2023) no.1, L8 doi:10.3847/2041-8213/acdac6 [arXiv:2306.16213 [astro-ph.HE]].
- [17] S. Vagnozzi, JHEAp **39** (2023), 81-98 doi:10.1016/j.jheap.2023.07.001 [arXiv:2306.16912 [astro-ph.CO]].
- [18] Z. Yi, Q. Gao, Y. Gong, Y. Wang and F. Zhang, Sci. China Phys. Mech. Astron. **66** (2023) no.12, 120404 doi:10.1007/s11433-023-2266-1 [arXiv:2307.02467 [gr-qc]].
- [19] S. Balaji, G. Domènech and G. Franciolini, JCAP **10** (2023), 041 doi:10.1088/1475-7516/2023/10/041 [arXiv:2307.08552 [gr-qc]].
- [20] V. K. Oikonomou, Phys. Rev. D **108** (2023) no.4, 043516 doi:10.1103/PhysRevD.108.043516 [arXiv:2306.17351 [astro-ph.CO]].
- [21] S. Nojiri, S. D. Odintsov and V. K. Oikonomou, Phys. Rept. **692** (2017) 1 [arXiv:1705.11098 [gr-qc]].
- [22] S. Capozziello, M. De Laurentis, Phys. Rept. **509**, 167 (2011);
V. Faraoni and S. Capozziello, Fundam. Theor. Phys. **170** (2010).
- [23] S. Nojiri, S.D. Odintsov, eConf **C0602061**, 06 (2006) [Int. J. Geom. Meth. Mod. Phys. **4**, 115 (2007)].
- [24] S. Nojiri, S.D. Odintsov, Phys. Rept. **505**, 59 (2011);
- [25] J. c. Hwang and H. Noh, Phys. Rev. D **71** (2005) 063536 doi:10.1103/PhysRevD.71.063536 [gr-qc/0412126].
- [26] S. Nojiri, S. D. Odintsov and M. Sami, Phys. Rev. D **74** (2006) 046004 doi:10.1103/PhysRevD.74.046004 [hep-th/0605039].
- [27] G. Cognola, E. Elizalde, S. Nojiri, S. Odintsov and S. Zerbini, Phys. Rev. D **75** (2007) 086002 doi:10.1103/PhysRevD.75.086002 [hep-th/0611198].
- [28] S. Nojiri, S. D. Odintsov and M. Sasaki, Phys. Rev. D **71** (2005) 123509 doi:10.1103/PhysRevD.71.123509 [hep-th/0504052].
- [29] S. Nojiri and S. D. Odintsov, Phys. Lett. B **631** (2005) 1 doi:10.1016/j.physletb.2005.10.010 [hep-th/0508049].
- [30] M. Satoh, S. Kanno and J. Soda, Phys. Rev. D **77** (2008) 023526 doi:10.1103/PhysRevD.77.023526 [arXiv:0706.3585 [astro-ph]].
- [31] K. Bamba, A. N. Makarenko, A. N. Myagky and S. D. Odintsov, JCAP **1504** (2015) 001 doi:10.1088/1475-7516/2015/04/001 [arXiv:1411.3852 [hep-th]].
- [32] Z. Yi, Y. Gong and M. Sabir, Phys. Rev. D **98** (2018) no.8, 083521 doi:10.1103/PhysRevD.98.083521 [arXiv:1804.09116 [gr-qc]].
- [33] Z. K. Guo and D. J. Schwarz, Phys. Rev. D **80** (2009) 063523 doi:10.1103/PhysRevD.80.063523 [arXiv:0907.0427 [hep-th]].
- [34] Z. K. Guo and D. J. Schwarz, Phys. Rev. D **81** (2010) 123520 doi:10.1103/PhysRevD.81.123520 [arXiv:1001.1897 [hep-th]].
- [35] P. X. Jiang, J. W. Hu and Z. K. Guo, Phys. Rev. D **88** (2013) 123508 doi:10.1103/PhysRevD.88.123508 [arXiv:1310.5579 [hep-th]].
- [36] C. van de Bruck, K. Dimopoulos, C. Longden and C. Owen, arXiv:1707.06839 [astro-ph.CO].
- [37] E. O. Pozdeeva, M. R. Gangopadhyay, M. Sami, A. V. Toporensky and S. Y. Vernov, Phys. Rev. D **102** (2020) no.4, 043525 doi:10.1103/PhysRevD.102.043525 [arXiv:2006.08027 [gr-qc]].
- [38] S. Vernov and E. Pozdeeva, Universe **7** (2021) no.5, 149 doi:10.3390/universe7050149 [arXiv:2104.11111 [gr-qc]].
- [39] E. O. Pozdeeva and S. Y. Vernov, Eur. Phys. J. C **81** (2021) no.7, 633 doi:10.1140/epjc/s10052-021-09435-8 [arXiv:2104.04995 [gr-qc]].
- [40] I. Fomin, Eur. Phys. J. C **80** (2020) no.12, 1145 doi:10.1140/epjc/s10052-020-08718-w [arXiv:2004.08065 [gr-qc]].
- [41] M. De Laurentis, M. Paoella and S. Capozziello, Phys. Rev. D **91** (2015) no.8, 083531 doi:10.1103/PhysRevD.91.083531 [arXiv:1503.04659 [gr-qc]].
- [42] Scalar Field Cosmology, S. Chervon, I. Fomin, V. Yurov and A. Yurov, World Scientific 2019, doi:10.1142/11405
- [43] K. Nozari and N. Rashidi, Phys. Rev. D **95** (2017) no.12, 123518 doi:10.1103/PhysRevD.95.123518 [arXiv:1705.02617 [astro-ph.CO]].
- [44] S. D. Odintsov and V. K. Oikonomou, Phys. Rev. D **98** (2018) no.4, 044039 doi:10.1103/PhysRevD.98.044039 [arXiv:1808.05045 [gr-qc]].
- [45] S. Kawai, M. a. Sakagami and J. Soda, Phys. Lett. B **437**, 284 (1998) doi:10.1016/S0370-2693(98)00925-3 [gr-qc/9802033].
- [46] Z. Yi and Y. Gong, Universe **5** (2019) no.9, 200 doi:10.3390/universe5090200 [arXiv:1811.01625 [gr-qc]].
- [47] C. van de Bruck, K. Dimopoulos and C. Longden, Phys. Rev. D **94** (2016) no.2, 023506 doi:10.1103/PhysRevD.94.023506 [arXiv:1605.06350 [astro-ph.CO]].
- [48] K. i. Maeda, N. Ohta and R. Wakebe, Eur. Phys. J. C **72** (2012) 1949 doi:10.1140/epjc/s10052-012-1949-6 [arXiv:1111.3251 [hep-th]].

- [49] W. Y. Ai, *Commun. Theor. Phys.* **72** (2020) no.9, 095402 doi:10.1088/1572-9494/aba242 [arXiv:2004.02858 [gr-qc]].
- [50] R. Easther and K. i. Maeda, *Phys. Rev. D* **54** (1996) 7252 doi:10.1103/PhysRevD.54.7252 [hep-th/9605173].
- [51] A. Codello and R. K. Jain, *Class. Quant. Grav.* **33** (2016) no.22, 225006 doi:10.1088/0264-9381/33/22/225006 [arXiv:1507.06308 [gr-qc]].
- [52] B. P. Abbott *et al.* [LIGO Scientific and Virgo], *Phys. Rev. Lett.* **119** (2017) no.16, 161101 doi:10.1103/PhysRevLett.119.161101 [arXiv:1710.05832 [gr-qc]].
- [53] B. P. Abbott *et al.* [LIGO Scientific, Virgo, Fermi-GBM and INTEGRAL], *Astrophys. J. Lett.* **848** (2017) no.2, L13 doi:10.3847/2041-8213/aa920c [arXiv:1710.05834 [astro-ph.HE]].
- [54] B. P. Abbott *et al.* “Multi-messenger Observations of a Binary Neutron Star Merger,” *Astrophys. J.* **848** (2017) no.2, L12 doi:10.3847/2041-8213/aa91c9 [arXiv:1710.05833 [astro-ph.HE]].
- [55] B. P. Abbott *et al.* [LIGO Scientific and Virgo], *Phys. Rev. D* **100** (2019) no.6, 061101 doi:10.1103/PhysRevD.100.061101 [arXiv:1903.02886 [gr-qc]].
- [56] J. M. Ezquiaga and M. Zumalacárregui, *Phys. Rev. Lett.* **119** (2017) no.25, 251304 doi:10.1103/PhysRevLett.119.251304 [arXiv:1710.05901 [astro-ph.CO]].
- [57] T. Baker, E. Bellini, P. G. Ferreira, M. Lagos, J. Noller and I. Sawicki, *Phys. Rev. Lett.* **119** (2017) no.25, 251301 doi:10.1103/PhysRevLett.119.251301 [arXiv:1710.06394 [astro-ph.CO]].
- [58] P. Creminelli and F. Vernizzi, *Phys. Rev. Lett.* **119** (2017) no.25, 251302 doi:10.1103/PhysRevLett.119.251302 [arXiv:1710.05877 [astro-ph.CO]].
- [59] J. Sakstein and B. Jain, *Phys. Rev. Lett.* **119** (2017) no.25, 251303 doi:10.1103/PhysRevLett.119.251303 [arXiv:1710.05893 [astro-ph.CO]].
- [60] S. Boran, S. Desai, E. O. Kahya and R. P. Woodard, *Phys. Rev. D* **97** (2018) no.4, 041501 doi:10.1103/PhysRevD.97.041501 [arXiv:1710.06168 [astro-ph.HE]].
- [61] V. K. Oikonomou, *Class. Quant. Grav.* **38** (2021) no.19, 195025 doi:10.1088/1361-6382/ac2168 [arXiv:2108.10460 [gr-qc]].
- [62] V. K. Oikonomou, *Astropart. Phys.* **141** (2022), 102718 doi:10.1016/j.astropartphys.2022.102718 [arXiv:2204.06304 [gr-qc]].
- [63] S. D. Odintsov, V. K. Oikonomou and F. P. Fronimos, *Nucl. Phys. B* **958** (2020), 115135 doi:10.1016/j.nuclphysb.2020.115135 [arXiv:2003.13724 [gr-qc]].
- [64] V. K. Oikonomou, *Phys. Rev. D* **103** (2021) no.12, 124028 doi:10.1103/PhysRevD.103.124028 [arXiv:2012.01312 [gr-qc]].
- [65] Y. Akrami *et al.* [Planck], *Astron. Astrophys.* **641** (2020), A10 doi:10.1051/0004-6361/201833887 [arXiv:1807.06211 [astro-ph.CO]].
- [66] P. A. R. Ade *et al.* [BICEP and Keck], *Phys. Rev. Lett.* **127** (2021) no.15, 151301 doi:10.1103/PhysRevLett.127.151301 [arXiv:2110.00483 [astro-ph.CO]].
- [67] M. Benetti, L. L. Graef and S. Vagnozzi, *Phys. Rev. D* **105** (2022) no.4, 043520 doi:10.1103/PhysRevD.105.043520 [arXiv:2111.04758 [astro-ph.CO]].
- [68] D. H. Lyth, *Phys. Rev. Lett.* **78** (1997), 1861-1863 doi:10.1103/PhysRevLett.78.1861 [arXiv:hep-ph/9606387 [hep-ph]].
- [69] E. Allys *et al.* [LiteBIRD], *PTEP* **2023** (2023) no.4, 042F01 doi:10.1093/ptep/ptac150 [arXiv:2202.02773 [astro-ph.IM]].
- [70] A. Caputo and G. Raffelt, *PoS COSMICWISPerS* (2024), 041 doi:10.22323/1.454.0041 [arXiv:2401.13728 [hep-ph]].
- [71] M. Kuster, G. Raffelt and B. Beltran, *Lect. Notes Phys.* **741** (2008), pp.1-258 doi:10.1007/978-3-540-73518-2
- [72] D. J. E. Marsh, *Phys. Rept.* **643** (2016), 1-79 doi:10.1016/j.physrep.2016.06.005 [arXiv:1510.07633 [astro-ph.CO]].
- [73] V. K. Oikonomou, P. Tsyba and O. Razina, *EPL* **145** (2024) no.4, 49001 doi:10.1209/0295-5075/ad239c [arXiv:2402.02049 [gr-qc]].
- [74] M. Kamionkowski and E. D. Kovetz, *Ann. Rev. Astron. Astrophys.* **54** (2016), 227-269 doi:10.1146/annurev-astro-081915-023433 [arXiv:1510.06042 [astro-ph.CO]].
- [75] M. S. Turner, M. J. White and J. E. Lidsey, *Phys. Rev. D* **48** (1993), 4613-4622 doi:10.1103/PhysRevD.48.4613 [arXiv:astro-ph/9306029 [astro-ph]].
- [76] L. A. Boyle and P. J. Steinhardt, *Phys. Rev. D* **77** (2008), 063504 doi:10.1103/PhysRevD.77.063504 [arXiv:astro-ph/0512014 [astro-ph]].
- [77] Y. Zhang, Y. Yuan, W. Zhao and Y. T. Chen, *Class. Quant. Grav.* **22** (2005), 1383-1394 doi:10.1088/0264-9381/22/7/011 [arXiv:astro-ph/0501329 [astro-ph]].
- [78] C. Caprini and D. G. Figueroa, *Class. Quant. Grav.* **35** (2018) no.16, 163001 doi:10.1088/1361-6382/aac608 [arXiv:1801.04268 [astro-ph.CO]].
- [79] T. J. Clarke, E. J. Copeland and A. Moss, *JCAP* **10** (2020), 002 doi:10.1088/1475-7516/2020/10/002 [arXiv:2004.11396 [astro-ph.CO]].
- [80] T. L. Smith, M. Kamionkowski and A. Cooray, *Phys. Rev. D* **73** (2006), 023504 doi:10.1103/PhysRevD.73.023504 [arXiv:astro-ph/0506422 [astro-ph]].
- [81] M. Giovannini, *Class. Quant. Grav.* **26** (2009), 045004 doi:10.1088/0264-9381/26/4/045004 [arXiv:0807.4317 [astro-ph]].
- [82] X. J. Liu, W. Zhao, Y. Zhang and Z. H. Zhu, *Phys. Rev. D* **93** (2016) no.2, 024031 doi:10.1103/PhysRevD.93.024031 [arXiv:1509.03524 [astro-ph.CO]].
- [83] M. Giovannini, [arXiv:2303.11928 [gr-qc]].
- [84] M. Giovannini, *Eur. Phys. J. C* **82** (2022) no.9, 828 doi:10.1140/epjc/s10052-022-10800-4 [arXiv:2206.08217 [gr-qc]].
- [85] M. Giovannini, *Phys. Rev. D* **105** (2022) no.10, 103524 doi:10.1103/PhysRevD.105.103524 [arXiv:2203.13586 [gr-qc]].
- [86] M. Giovannini, *Phys. Lett. B* **810** (2020), 135801 doi:10.1016/j.physletb.2020.135801 [arXiv:2006.02760 [gr-qc]].
- [87] M. Giovannini, *Prog. Part. Nucl. Phys.* **112** (2020), 103774 doi:10.1016/j.pnpnp.2020.103774 [arXiv:1912.07065 [astro-ph.CO]].

- [88] M. Giovannini, Phys. Rev. D **100** (2019) no.8, 083531 doi:10.1103/PhysRevD.100.083531 [arXiv:1908.09679 [hep-th]].
- [89] M. Giovannini, Phys. Rev. D **91** (2015) no.2, 023521 doi:10.1103/PhysRevD.91.023521 [arXiv:1410.5307 [hep-th]].
- [90] M. Giovannini, PMC Phys. A **4** (2010), 1 doi:10.1186/1754-0410-4-1 [arXiv:0901.3026 [astro-ph.CO]].
- [91] M. Kamionkowski, A. Kosowsky and M. S. Turner, Phys. Rev. D **49** (1994), 2837-2851 doi:10.1103/PhysRevD.49.2837 [arXiv:astro-ph/9310044 [astro-ph]].
- [92] W. Giarè and F. Renzi, Phys. Rev. D **102** (2020) no.8, 083530 doi:10.1103/PhysRevD.102.083530 [arXiv:2007.04256 [astro-ph.CO]].
- [93] W. Zhao and Y. Zhang, Phys. Rev. D **74** (2006), 043503 doi:10.1103/PhysRevD.74.043503 [arXiv:astro-ph/0604458 [astro-ph]].
- [94] P. D. Lasky, C. M. F. Mingarelli, T. L. Smith, J. T. Giblin, D. J. Reardon, R. Caldwell, M. Bailes, N. D. R. Bhat, S. Burke-Spolaor and W. Coles, *et al.* Phys. Rev. X **6** (2016) no.1, 011035 doi:10.1103/PhysRevX.6.011035 [arXiv:1511.05994 [astro-ph.CO]].
- [95] R. G. Cai, C. Fu and W. W. Yu, [arXiv:2112.04794 [astro-ph.CO]].
- [96] S. D. Odintsov, V. K. Oikonomou and F. P. Fronimos, Phys. Dark Univ. **35** (2022), 100950 doi:10.1016/j.dark.2022.100950 [arXiv:2108.11231 [gr-qc]].
- [97] J. Lin, S. Gao, Y. Gong, Y. Lu, Z. Wang and F. Zhang, [arXiv:2111.01362 [gr-qc]].
- [98] F. Zhang, J. Lin and Y. Lu, Phys. Rev. D **104** (2021) no.6, 063515 [erratum: Phys. Rev. D **104** (2021) no.12, 129902] doi:10.1103/PhysRevD.104.063515 [arXiv:2106.10792 [gr-qc]].
- [99] L. Visinelli, N. Bolis and S. Vagnozzi, Phys. Rev. D **97** (2018) no.6, 064039 doi:10.1103/PhysRevD.97.064039 [arXiv:1711.06628 [gr-qc]].
- [100] J. R. Pritchard and M. Kamionkowski, Annals Phys. **318** (2005), 2-36 doi:10.1016/j.aop.2005.03.005 [arXiv:astro-ph/0412581 [astro-ph]].
- [101] V. V. Khoze and D. L. Milne, [arXiv:2212.04784 [hep-ph]].
- [102] A. Casalino, M. Rinaldi, L. Sebastiani and S. Vagnozzi, Phys. Dark Univ. **22** (2018), 108 doi:10.1016/j.dark.2018.10.001 [arXiv:1803.02620 [gr-qc]].
- [103] A. Casalino, M. Rinaldi, L. Sebastiani and S. Vagnozzi, Class. Quant. Grav. **36** (2019) no.1, 017001 doi:10.1088/1361-6382/aaf1fd [arXiv:1811.06830 [gr-qc]].
- [104] K. El Bourakadi, B. Asfour, Z. Sakhi, Z. M. Bennai and T. Ouali, Eur. Phys. J. C **82** (2022) no.9, 792 doi:10.1140/epjc/s10052-022-10762-7 [arXiv:2209.08585 [gr-qc]].
- [105] R. Sturani, Symmetry **13** (2021) no.12, 2384 doi:10.3390/sym13122384
- [106] S. Vagnozzi and A. Loeb, Astrophys. J. Lett. **939** (2022) no.2, L22 doi:10.3847/2041-8213/ac9b0e [arXiv:2208.14088 [astro-ph.CO]].
- [107] A. S. Arapoğlu and A. E. Yükselci, [arXiv:2210.16699 [gr-qc]].
- [108] W. Giarè, M. Forconi, E. Di Valentino and A. Melchiorri, [arXiv:2210.14159 [astro-ph.CO]].
- [109] M. Gerbino, K. Freese, S. Vagnozzi, M. Lattanzi, O. Mena, E. Giusarma and S. Ho, Phys. Rev. D **95** (2017) no.4, 043512 doi:10.1103/PhysRevD.95.043512 [arXiv:1610.08830 [astro-ph.CO]].
- [110] M. Breitbach, J. Kopp, E. Madge, T. Opferkuch and P. Schwaller, JCAP **07** (2019), 007 doi:10.1088/1475-7516/2019/07/007 [arXiv:1811.11175 [hep-ph]].
- [111] S. Pi, M. Sasaki and Y. I. Zhang, JCAP **06** (2019), 049 doi:10.1088/1475-7516/2019/06/049 [arXiv:1904.06304 [gr-qc]].
- [112] M. Khlopov and S. R. Chowdhury, Symmetry **15** (2023) no.4, 832 doi:10.3390/sym15040832
- [113] S. D. Odintsov, V. K. Oikonomou and R. Myrzakulov, Symmetry **14** (2022) no.4, 729 doi:10.3390/sym14040729 [arXiv:2204.00876 [gr-qc]].
- [114] S. Vagnozzi, Mon. Not. Roy. Astron. Soc. **502** (2021) no.1, L11-L15 doi:10.1093/mnras/slaa203 [arXiv:2009.13432 [astro-ph.CO]].
- [115] S. Pi, M. Sasaki, A. Wang and J. Wang, Phys. Rev. D **110** (2024) no.10, 103529 doi:10.1103/PhysRevD.110.103529 [arXiv:2407.06066 [astro-ph.CO]].
- [116] V. K. Oikonomou, P. Tsyba and O. Razina, Annals Phys. **462** (2024), 169597 doi:10.1016/j.aop.2024.169597 [arXiv:2401.11273 [gr-qc]].